

A Quantile Approach to Evaluating Asset Pricing Models

Tjeerd de Vries ^{*}

This Version: September 21, 2022

First draft: June 2021

Abstract

This paper studies the misspecification of asset pricing models using a local measure of dependence between the stochastic discount factor (SDF) and market return. I propose a bound on the volatility of the SDF that is stronger than the [Hansen and Jagannathan \(1991\)](#) bound, due to local differences between the physical and risk-neutral distribution in the left tail. Using quantile regression, I show that this conclusion continues to hold based on conditional information. Finally, I propose a lower bound on the physical quantile which is approximately tight in the data. I interpret the bound as a real time measure of the Peso problem and find that it fluctuates significantly over time. At the height of the 2008 financial crisis and 2020 Covid crisis, my bound predicts that a market return of -28% or lower has a 5% probability. Both findings provide model-free evidence for time varying disaster risk.

Keywords: Asset pricing, Model misspecification, Quantile methods

JEL Codes: G13, G17, C14, C22

^{*}Department of Economics, University of California San Diego. Email: tjdevrie@ucsd.edu. I would like to thank Alexis Toda, Allan Timmermann, James Hamilton, Xinwei Ma, Yixiao Sun, Rossen Valkanov, Brendan Beare, Caio Almeida and participants of the 2022 SoFiE conference for useful feedback. All errors are my own.

1 Introduction

Evaluating the misspecification of asset pricing models is crucial for understanding the shortcomings of a particular modeling approach. For example, Hansen and Jagannathan (1991) (HJ henceforth) show that the Sharpe ratio puts a tight lower bound on the unobserved volatility of the stochastic discount factor (SDF). Subsequently, new bounds have been proposed that use asset returns to bound moments of the unobserved SDF (Snow, 1991; Stutzer, 1995; Bansal and Lehmann, 1997; Alvarez and Jermann, 2005; Bakshi and Chabi-Yo, 2012; Almeida and Garcia, 2012; Backus et al., 2014; Liu, 2021). Altogether, these bounds enhance our understanding of why a model is misspecified and along which dimension we must improve its fit.

In this paper, I propose a new way to analyze model misspecification based on *local information*. This approach departs from the existing literature above, which uses bounds based on global information such as the Sharpe ratio. Roughly speaking, bounds based on higher order moments are global, since they use information from the entire distribution of returns. In contrast, this paper uses quantiles as a local measure of information to bound unobserved moments of the SDF. I show that there is a close connection between the global and local approach, in the sense that the HJ bound can be understood as an average of my local bound over the state space.

This local approach has several distinct advantages. First, I show that my bound on the SDF volatility, referred to as the *quantile bound*, locally measures the difference between the physical and risk-neutral distribution. In the data, this difference is most pronounced around the 5th percentile, which implies an SDF volatility of at least 30%. In contrast, the Sharpe ratio renders a much looser bound on the SDF volatility, of about 13%. I interpret this finding as favorable evidence for models that embed disaster risk, since these models imply that the physical and risk-neutral distribution locally differ most in the left tail. A global bound such as the Sharpe ratio does not reveal this local dispersion.

Second, the shape of the quantile bound is a useful model diagnostic, as it pinpoints which part of the return distribution is most misspecified. For example, asset pricing models that assume joint lognormality imply that the quantile bound is almost symmetric around the median and steeply decreasing in both tails. In contrast, the data show that the quantile bound is highly asymmetric and low around the median, which can be taken as evidence against the lognormal assumption.

Third, I use this local analysis to uncover other stylized facts of the data based on conditional information. Conditional on time t , it is possible to identify the risk-

neutral distribution from option prices. However, asset prices cannot directly be used to estimate the physical distribution, at least nonparametrically. I overcome this problem by running quantile regressions of the risk-neutral quantile on the realized return. Importantly, both the realized return and the risk-neutral distribution are forward looking and thus belong to the same information set.¹ Quantile regression then allows me to measure how well the risk-neutral distribution fits the physical distribution in different parts of the support. I find that the risk-neutral distribution approximates the physical distribution well in the right tail, *but not in the left tail*. This evidence is consistent with time varying disaster risk models (Gabaix, 2012; Wachter, 2013). Moreover, the evidence also shows that the right tail of the physical distribution can be recovered approximately from the risk-neutral distribution. Incidentally, this approach also renders model-free evidence against pricing kernel monotonicity, in a way that properly accounts for conditional information and without the need to estimate the physical distribution.

Fourth, since most of my empirical results point to disaster risk in the data, I propose a model-free way to measure time varying disaster risk, which is also based on quantiles. Martin (2013) points out that disaster risk models are notoriously hard to calibrate due to the infrequent occurrence of disaster shocks. Hence, most evidence for disaster risk is indirect. I use the risk-neutral quantile, together with a risk-adjustment term, to approximate the latent physical quantile function. This risk-adjustment term derives from option prices and is nonparametric. Using quantile regression, I show that the risk-adjustment term captures most of the (unobserved) wedge between the physical and risk-neutral quantile function. Since the left tail of the physical quantile function is a good measure of disaster risk, I thus obtain a market observed proxy for disaster risk. I show that my measure of disaster risk aligns well with events associated to high market uncertainty such as the 2008 financial crisis or the 2020 Covid pandemic. At the height of these periods, my measure predicts that with 5% probability, the (monthly) market return would drop by 28% or more. This probability is 57 times higher than historical data suggest, thereby giving direct evidence of disaster risk. I also find that the disaster risk measure fluctuates significantly over time, which is model-free evidence for time varying disaster risk.

Finally, I propose several out-of-sample exercises to assess the robustness of my findings. The literature on predicting excess returns stresses the importance of out-of-sample performance (Campbell and Thompson, 2008; Welch and Goyal, 2008), but many of the performance measures such as the out-of-sample R^2 are tailored

¹Linn et al. (2018) emphasize this point and argue that a mismatch of information can lead to inconsistent estimates.

to OLS and not applicable to quantile regression. I propose a clean substitute for the out-of-sample R^2 in the context of quantile regression. Using this out-of-sample measure, I find that the risk-adjustment term better predicts the physical quantile than competing benchmarks. In contrast to the equity premium, the literature offers little guidance on variables that should predict quantiles. I consider one natural benchmark, namely the VIX index, since it is available at a daily frequency and it is known to correlate with negative market sentiment (Bekaert and Hoerova, 2014). Surprisingly, in the left tail, the risk-adjustment term outperforms the VIX predictor, which uses in-sample information. This fact lends credit to our interpretation of the risk-adjustment term as disaster risk, since this term does not require estimation of any parameters. I obtain the same result in the right tail of the return distribution, using the risk-neutral quantile as a predictor.

Related literature. This paper contributes to the literature on model misspecification in asset pricing. Hansen and Jagannathan (1991) derive a nonparametric bound on the SDF volatility and use it to establish a duality relation with the maximum Sharpe ratio. Many researchers followed up with higher order bounds (Snow, 1991; Almeida and Garcia, 2012; Liu, 2021) and entropy bounds (Stutzer, 1995; Bansal and Lehmann, 1997; Alvarez and Jermann, 2005; Backus et al., 2014). All these bounds can be used to screen candidate asset pricing models. Theoretically, these bounds give some measure how much the risk-neutral distribution differs from the physical distribution. All these measures are global in the sense of using a functional of the physical expectation. In contrast, I focus on bounds using local information through the use of quantiles.

My bound relies on the physical CDF and risk-neutral quantile function, both of which can be estimated from historical return and option data. Aït-Sahalia and Lo (1998, 2000), Jackwerth (2000), Rosenberg and Engle (2002) and Cuesdeanu and Jackwerth (2018) consider nonparametric estimates of the entire SDF, which is the ratio of the risk-neutral density to the physical density. Although my approach only renders a lower bound on the SDF volatility, this lower bound is easier to estimate than a ratio of densities because I only require a CDF and the quantile function, which can typically be estimated at a faster rate. Moreover, the bound derived in this paper is used to diagnose model misspecification, which is rather different from the application in the aforementioned papers.

This paper also connects to the burgeoning literature on using options to obtain forward looking estimates of the equity premium (Martin, 2017; Martin and Wagner, 2019; Chabi-Yo and Loudis, 2020). However, instead of focusing on the conditional

expectation of excess returns, I use option data to predict conditional return quantiles. The relation between option prices and expected shocks to the market return has received a great deal of attention, see for example [Bates \(1991, 2000, 2008\)](#), [Coval and Shumway \(2001\)](#), [Bollerslev and Todorov \(2011\)](#), [Backus et al. \(2011\)](#) and [Ross \(2015\)](#). Similar to [Bollerslev and Todorov \(2011\)](#), I obtain a nonparametric measure of fear or disaster risk. My approach differs in that I only use risk-neutral information and the theoretical motivation comes from the interplay between the physical and risk-neutral quantile function. I build on [Chabi-Yo and Loudis \(2020\)](#) and extend their results to approximate the wedge between the physical and risk-neutral quantile function in the left tail. This approach also complements the recovery literature ([Ross, 2015](#); [Borovička et al., 2016](#); [Qin and Linetsky, 2017](#)), since I derive forward looking approximations to the left and right tail of the physical distribution using option data. The time variation in my approximation for the left tail quantile is consistent with the time varying disaster risk models of [Gabaix \(2012\)](#) and [Wachter \(2013\)](#).

Finally, I build on the equity premium literature to analyze the out-of-sample performance of my measure of disaster risk. The evaluation and performance of conditional expected return predictors is well understood in the literature, especially after fundamental contributions of [Campbell and Thompson \(2008\)](#) and [Welch and Goyal \(2008\)](#). I draw on earlier work of [Koenker and Machado \(1999\)](#) and extend the evaluation toolkit to the quantile setting, specifically out-of-sample. My work thus complements the literature on conditional return prediction and extends it to the whole distribution.

The rest of this paper is organized as follows. Section 2 introduces the quantile bound and discusses its use in asset pricing models, Section 3 estimates the quantile bound with actual data. Section 4 extends the empirical results using conditional information. Finally, Section 5 concludes.

2 Quantile bound on the SDF volatility and model implications

2.1 Notation

Let R be the return on any tradable asset and their portfolios. Throughout I assume no-arbitrage, which implies the existence of a positive stochastic discount factor

(SDF) denoted by M , such that

$$\mathbb{E}[MR] = 1. \quad (2.1)$$

The expectation in (2.1) is taken with respect to a probability measure \mathbb{P} , frequently referred to as the physical measure, which represents the true probability distribution of the data generating process. Alternatively, the relation in (2.1) can be reformulated in terms of the risk-neutral measure. That is, there exists a probability measure $\tilde{\mathbb{P}}$ equivalent to \mathbb{P} such that²

$$\tilde{\mathbb{E}}[R] = 1/\mathbb{E}[M]. \quad (2.2)$$

The expectation on the left in (2.2) is taken with respect to $\tilde{\mathbb{P}}$. Throughout the paper, I use tilde (\sim) to denote random variables that are calculated under the risk-neutral measure $\tilde{\mathbb{P}}$. If we assume the existence of a risk-free asset with return R_f , then $\mathbb{E}[M] = 1/R_f$. Mathematically, the connection between (2.1) and (2.2) follows since $M/\mathbb{E}[M]$ is the Radon-Nikodym derivative of the measures \mathbb{P} and $\tilde{\mathbb{P}}$. The SDF can potentially depend on many state variables. To avoid having to specify or estimate these state variables, I work with the projected SDF

$$M = \mathbb{E}[M^*|R],$$

where M^* is the SDF that depends on all the state variables. The projected SDF has the same pricing implications for contingent claims written on the observed return (Cochrane, 2005, pp. 66–67).³

2.2 Quantile bound

I now derive a bound on the SDF volatility that shows how any pointwise difference between the physical and risk-neutral distribution leads to a volatile SDF. Before stating the bound, I introduce $\tilde{F}(\cdot)$ (resp. $F(\cdot)$) to denote the risk-neutral (resp. physical) CDF and write $\tilde{Q}_\tau(R)$ to denote the risk-neutral τ -quantile of the return R . I omit R and write \tilde{Q}_τ whenever the dependence on R is clear from the context. By definition, the risk-neutral quantile function satisfies

$$\tilde{F}(\tilde{Q}_\tau(R)) := \tilde{\mathbb{P}}(R \leq \tilde{Q}_\tau) = \tau.$$

For ease of notation, I also define $\phi(\tau) := F(\tilde{Q}_\tau(R))$, which can be interpreted as the ordinal dominance curve of the measures \mathbb{P} and $\tilde{\mathbb{P}}$ (Hsieh and Turnbull, 1996). Finally, let $\aleph^+ := \{M : M \geq 0 \text{ and } \mathbb{E}(MR) = 1\}$, the space of all nonnegative SDFs

²Two probability measures \mathbb{P} and $\tilde{\mathbb{P}}$ are said to be equivalent whenever $\mathbb{P}(A) = 0 \iff \tilde{\mathbb{P}}(A) = 0$.

³Formally, M is a measurable function of R , but I do not denote this dependence explicitly to simplify notation.

([Hansen and Jagannathan, 1991](#)). The new SDF volatility bound can now be stated as follows.

Theorem 2.1 (Quantile bound). *Assume no-arbitrage, then for any $M \in \mathbb{N}^+$, we have*

$$\frac{\sigma(M)}{\mathbb{E}[M]} \geq \frac{|\tau - \phi(\tau)|}{\sqrt{\phi(\tau)(1 - \phi(\tau))}} \quad \forall \tau \in (0, 1). \quad (2.3)$$

If a risk-free asset exists, then $\mathbb{E}[M] = 1/R_f$ and (2.3) simplifies to

$$\sigma(M) \geq \frac{|\tau - \phi(\tau)|}{\sqrt{\phi(\tau)(1 - \phi(\tau))} R_f} \quad \forall \tau \in (0, 1). \quad (2.4)$$

Proof. See Appendix [A.1](#). ■

I refer to Theorem [2.1](#) as the quantile bound, since a key ingredient in (2.3) is the risk-neutral quantile function. If $\mathbb{P} = \tilde{\mathbb{P}}$, agents are risk-neutral and the dominance curve evaluates to $\phi(\tau) = \tau$. In that case the quantile bound degenerates to zero. Theorem [2.1](#) makes precise the sense in which any difference between the physical and risk-neutral distribution leads to a volatile SDF. Compare this to the classical HJ bound:

$$\sigma(M) \geq \frac{|\mathbb{E}(R) - R_f|}{\sigma(R)R_f}. \quad (2.5)$$

The lower bound in (2.5) shows that any excess return leads to a volatile SDF. Essentially, (2.5) uses three sources of information: (i) The mean of the physical distribution (ii) The mean of the risk-neutral distribution (iii) The variance of the physical distribution. The lower bound in (2.5) is also a global measure of distance between \mathbb{P} and $\tilde{\mathbb{P}}$, since the mean and volatility are averages across the whole distribution.

In contrast, the bound in (2.3) compares the physical and risk-neutral distribution for every τ -quantile, which is a *local* measure of distance between \mathbb{P} and $\tilde{\mathbb{P}}$. To clarify this local interpretation, I use a classical result of Hoeffding (see Appendix [A.3](#))

$$\mathbb{C}\mathbb{O}\mathbb{V}[R, M] = - \int_{-\infty}^{\infty} \mathbb{C}\mathbb{O}\mathbb{V}[\mathbb{1}(R \leq x), M] dx. \quad (2.6)$$

Equation (2.6) shows that $\mathbb{C}\mathbb{O}\mathbb{V}[\mathbb{1}(R \leq x), M]$ locally measures the dependence between the SDF and return. The average over all local measures is equal to the global measure of dependence given by $\mathbb{C}\mathbb{O}\mathbb{V}[R, M]$. HJ apply the Cauchy-Schwarz inequality to $\mathbb{C}\mathbb{O}\mathbb{V}[R, M]$, in order to derive their bound on the SDF volatility. In contrast, I apply Cauchy-Schwarz to the local measure of dependence, $\mathbb{C}\mathbb{O}\mathbb{V}[\mathbb{1}(R \leq \tilde{Q}_\tau), M]$. This local measure is expected to yield sharper bounds on the SDF volatility if, for

example, there is high tail dependence between the SDF and return.⁴

If there is no priced jump or stochastic volatility risk, $\phi(\tau)$ is determined by the equity premium and the HJ bound in (2.5) captures all relevant information. On the other hand, if there are risk premia for jumps or stochastic volatility, the measures \mathbb{P} and $\tilde{\mathbb{P}}$ differ both in shape and location (Broadie et al., 2009), which implies that $\phi(\tau)$ contains information that is not captured by the HJ bound. Moreover, the quantile bound is robust to fat-tails, since it is well defined regardless of any moment restrictions on the returns. Fat-tails and other higher order shape restrictions such as negative skewness are essential features of financial return data (Gao and Martin, 2021).

Finally, the quantile bound can also be understood as a Sharpe ratio on selling insurance against crash risk, for small values of τ . Consider a security that pays out \$1 whenever the asset return is below \tilde{Q}_τ for some small τ . The price of such a security is given by

$$\mathbb{E}[M] \tilde{\mathbb{E}} \left[\mathbb{1}(R \leq \tilde{Q}_\tau) \right] = \mathbb{E}[M] \tau. \quad (2.7)$$

Similarly, the (discounted) expected return is

$$\mathbb{E}[M] \mathbb{E} \left[\mathbb{1}(R \leq \tilde{Q}_\tau) \right] = \mathbb{E}[M] \phi(\tau). \quad (2.8)$$

And the risk associated with this investment is given by

$$\sigma \left(\mathbb{1}(R \leq \tilde{Q}_\tau) \right) = \sqrt{\phi(\tau)(1 - \phi(\tau))}. \quad (2.9)$$

Combining (2.7), (2.8) and (2.9) to form the Sharpe ratio we recover the right hand side of (2.3). This interpretation is useful when I analyze the difference between the HJ and quantile bound for disaster risk models. The class of disaster risk models posits that high Sharpe ratios on the market portfolio are driven by investor's fear of extreme (negative) shocks to consumption. Following this reasoning, we expect high Sharpe ratios for small quantiles in (2.3), due to the crash risk interpretation. In this sense, the quantile bound is a more direct measure of the influence of disasters on the behavior of the SDF. I formalize this argument in the next section using the disaster risk calibration of Backus et al. (2011).

2.3 Quantile and HJ bound in asset pricing models

In this section, I compare the quantile bound to the HJ bound in (common) asset pricing models. It turns out that the quantile bound is always weaker than the

⁴See McNeil et al. (2015, Chapter 7.2.4) for a formal definition of tail dependence.

HJ bound in models that assume normality. More generally, I show that lognormal models have difficulty to produce a stronger quantile bound, but disaster risk models do not. This finding puts an additional constraint on asset pricing models, since real data in Section 3.2 show that the quantile bound is significantly stronger than the HJ bound. Appendix D contains similar results in this direction using other well known asset pricing bounds.

Example 2.1 (CAPM). The Capital Asset Pricing Model (CAPM) specifies the SDF as

$$M = \alpha - \beta R_m.$$

Here, R_m denotes the return on the market portfolio. In this case $M \notin \mathbb{N}^+$, since the SDF can become negative. However, this probability is very small over short time horizons or we can think of M as an approximation to $M^* := \max(0, M) \in \mathbb{N}^+$. Since the HJ bound is derived by applying the Cauchy-Schwarz inequality to $\text{COV}(R_m, M)$, the inequality binds if M is a linear combination of R_m . Hence, under CAPM, the HJ bound is strictly stronger than the quantile bound regardless of the distribution of R_m .

Example 2.2 (Joint normality). Suppose that M and R are jointly normally distributed and denote the mean and variance of R by μ_R and σ_R^2 respectively. The normality assumption violates no-arbitrage since M can be negative, but could be defended as an approximation over short time horizons when the variance is small (see Example 2.3). In Appendix A.3, I prove that

$$\left| \text{COV} \left(\mathbb{1} \left(R \leq \tilde{Q}_\tau \right), M \right) \right| = f_R(\tilde{Q}_\tau) |\text{COV}(R, M)|, \quad (2.10)$$

where $f_R(\cdot)$ is the marginal density of R .⁵ This identity gives an explicit expression for the weighting factor in Hoeffding's identity (2.6). In Appendix A.3, I also derive an explicit expression for the relative efficiency between the quantile and HJ bound

$$\frac{\text{HJ bound}}{\text{Quantile bound}} = \frac{\sqrt{\phi(\tau)(1 - \phi(\tau))}}{\sigma_R f_R(\tilde{Q}_\tau)}. \quad (2.11)$$

To see that the HJ bound is always stronger than the quantile bound, minimize (2.11) with respect to τ . We can show that the minimizer τ^* satisfies $\tilde{Q}_{\tau^*} = \mu_R$.⁶ For this choice, $\phi(\tau^*) = \mathbb{P}(R \leq \tilde{Q}_{\tau^*}) = 1/2$ and $f_R(\tilde{Q}_{\tau^*}) = 1/\sqrt{2\pi\sigma_R^2}$. Therefore,

⁵Notice that this is the marginal density under physical measure \mathbb{P} .

⁶To see this, write $x = \tilde{Q}_\tau$, and use $F(\cdot)$ to denote the physical CDF of R . I also drop the R subscript for f to avoid notational clutter. Consider

$$\Gamma(x) = \frac{F(x)(1 - F(x))}{f(x)^2}.$$

Minimizing $\Gamma(x)$ is equivalent to minimizing (2.11) and first order conditions imply that the optimal

(2.11) obeys the bound

$$\frac{\sqrt{\phi(\tau)(1-\phi(\tau))}}{\sigma_R f(\tilde{Q}_\tau)} \geq \frac{\sqrt{2\pi}}{2} \approx 1.25.$$

Hence, the HJ bound is always stronger in a model where the SDF and return are jointly normal.

In the following example, I need Stein's Lemma (Casella and Berger, 2002, Lemma 3.6.5):⁷

Lemma 2.2 (Stein's Lemma). *If X_1, X_2 are bivariate normal, $g : \mathbb{R} \rightarrow \mathbb{R}$ is differentiable and $\mathbb{E}|g'(X_1)| < \infty$, then*

$$\text{COV}(g(X_1), X_2) = \mathbb{E}[g'(X_1)] \text{COV}(X_1, X_2).$$

Example 2.3 (Joint lognormality). Let Z_R and Z_M be standard normal random variables with correlation ρ and consider the specification

$$\begin{aligned} R &= e^{(\mu_R - \frac{\sigma_R^2}{2})\lambda + \sigma_R \sqrt{\lambda} Z_R} \\ M &= e^{-(r_f + \frac{\sigma_M^2}{2})\lambda + \sigma_M \sqrt{\lambda} Z_M}, \end{aligned}$$

where λ governs the time scale. Simple algebra shows that the no-arbitrage condition, $\mathbb{E}[RM] = 1$, is satisfied when $\mu_R - r_f = -\rho\sigma_R\sigma_M$. It is hard to find an analytical solution for the relative efficiency between the HJ and quantile bound in this case, but linearization leads to a closed form expression which is accurate in simulations. The details are described in Appendix A.4, where I prove that

$$\min_{\tau \in (0,1)} \frac{\text{HJ bound}}{\text{Quantile bound}} \approx \frac{1}{2} \sqrt{\frac{2\pi\sigma_R^2\lambda}{\exp(\sigma_R^2\lambda) - 1}}. \quad (2.13)$$

This expression is independent of μ_R . An application of l'Hôpital's rule reveals that the relative efficiency converges to $\sqrt{2\pi}/2$ if $\lambda \rightarrow 0^+$. This is the same relative efficiency in Example 2.2, which is unsurprising as the linearization becomes exact in the limit as $\lambda \rightarrow 0^+$. The ratio in (2.13) is less than 1 if $\sigma \geq 0.92$ and $\lambda = 1$. In practice, annualized market return volatility is about 16%, which means that the HJ bound is stronger than the quantile bound under any reasonable parameterization if

x^* satisfies

$$[f(x^*) - 2F(x^*)f(x^*)]f(x^*)^2 - 2f(x^*)f'(x^*)[F(x^*)(1 - F(x^*))] = 0. \quad (2.12)$$

Since f, F are the respective PDF and CDF of the normal random variable R , it follows that $f'(\mu_R) = 0$ and $F(\mu_R) = 1/2$. As a result, (2.12) holds when $\tilde{Q}_{\tau^*} = x^* = \mu_R$.

⁷I use the form of Stein's Lemma reported in Cochrane (2005, p. 163), which follows from Stein's lemma as reported in Casella and Berger (2002).

the SDF and asset return are lognormal.

Example 2.4 (Pareto distribution). I now give an example of a model where the quantile bound can be stronger than the HJ bound, due to the fat tails of the return distribution. Let $U \sim \mathbf{Unif}[0, 1]$ (Uniform distribution on $[0, 1]$) and consider the following specification:

$$M = AU^\alpha, \quad R = BU^{-\beta} \quad \text{with} \quad \alpha, \beta, A, B > 0. \quad (2.14)$$

A random variable $X \sim \mathbf{Par}(C, \zeta)$ follows a Pareto distribution with scale parameter $C > 0$ and shape parameter $\zeta > 0$ if the CDF is given by

$$\mathbb{P}(X \leq x) = \begin{cases} 1 - (x/C)^{-\zeta} & x \geq C \\ 0 & x < C. \end{cases}$$

The assumption (2.14) implies that returns follow a Pareto distribution, both under the physical and risk-neutral measure. This fact allows me to obtain an explicit expression for the quantile bound. I summarize these properties in the Proposition below.

Proposition 2.3. *Let the SDF and return be given by (2.14). Then,*

- (i) *Under \mathbb{P} , the distribution of returns is Pareto: $R \sim \mathbf{Par}(B, 1/\beta)$.*
- (ii) *Under $\tilde{\mathbb{P}}$, the distribution of returns is Pareto: $R \sim \mathbf{Par}\left(B, \frac{\alpha+1}{\beta}\right)$.*
- (iii) *The Sharpe ratio on the asset return is given by*

$$\frac{\mathbb{E}[R] - R_f}{\sigma(R)} = \frac{\frac{B}{1-\beta} - \frac{\alpha+1}{A}}{\sqrt{\frac{B^2}{1-2\beta} - \left(\frac{B}{1-\beta}\right)^2}}. \quad (2.15)$$

- (iv) *The quantile bound is given by*

$$\frac{1}{R_f} \frac{|\tau - \phi(\tau)|}{\sqrt{\phi(\tau)(1 - \phi(\tau))}} = \frac{A}{1 + \alpha} \frac{|\tau - 1 + (1 - \tau)^{\frac{1}{\alpha+1}}|}{\sqrt{(1 - (1 - \tau)^{\frac{1}{\alpha+1}})(1 - \tau)^{\frac{1}{\alpha+1}}}}.$$

- (v) *If $\beta \uparrow \frac{1}{2}$, then the HJ bound converges to 0.*

Proof. See Appendix A.2. ■

Proposition 2.3 shows that the quantile bound is independent of the Pareto tail index β . Properties (iv) and (v) provide some intuition when the quantile bound is stronger than the HJ bound. Namely, heavier tails of the distribution of R (as

measured by β) lead to a lower Sharpe ratio. However, the quantile bound is unaffected by β since it only depends on the tail index α . Therefore, when β gets close to $1/2$, the HJ bound is rather uninformative whereas the quantile bound may fare better. Moreover, we do not need to impose any restrictions on the parameter space to calculate the quantile bound, while the HJ bound requires $\beta < 1/2$.⁸

Figure 1 shows two instances of the quantile and HJ bound using different parameter calibrations. Both calibrations are targeted to match an equity premium of 8% and risk-free rate of 0%. However, in Panel (b), the distribution of returns has a fatter tail compared to Panel (a). In both calibrations, the quantile bound has a range of values for which it is stronger than the HJ bound. In line with Proposition 2.3, we see that the range is larger in Panel (b), since the HJ bound is less informative owing to the heavier tails of R .

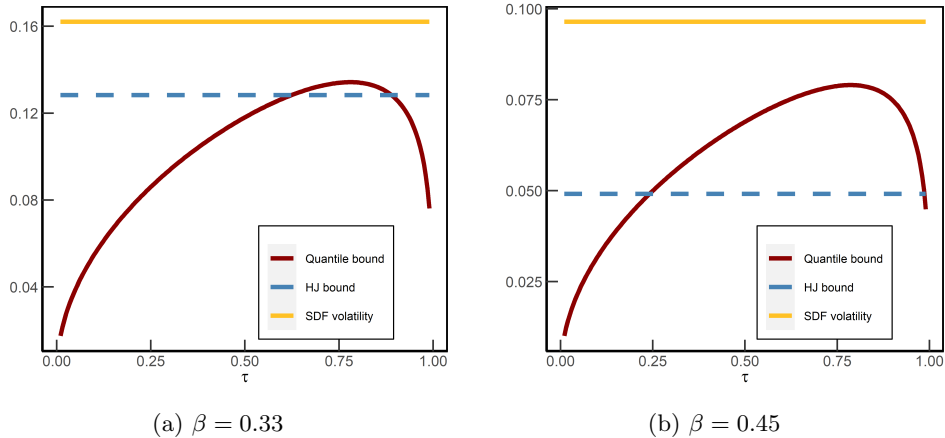


Figure 1: **Quantile and HJ bound for heavy tailed returns.** Both panels plot the quantile bound, HJ bound and true SDF volatility for the Pareto model (2.14). In Panel (b), the distribution of returns has a fatter tail compared to Panel (a). Panel (a) uses the parameters $[A, \alpha, B, \beta] = [1.19, 0.19, 0.72, 0.33]$. Panel (b) uses the parameters $[A, \alpha, B, \beta] = [1.11, 0.11, 0.59, 0.45]$. Both calibrations imply an equity premium of 8% and (net) risk-free rate of 0%.

Example 2.5 (Disaster risk). The disaster risk model of [Rietz \(1988\)](#) and [Barro \(2006\)](#) posits that risk premia are driven by extreme events that affect consumption growth. I follow the specification in [Backus et al. \(2011\)](#), who assume that the representative agent has power utility and the log pricing kernel is given by

$$\log M = \log(\beta) - \gamma \Delta c.$$

⁸The latter restriction is not unreasonable for asset returns, since typical tail index estimates suggest $\beta \in [1/4, 1/3]$ ([Danielsson and de Vries, 2000](#)).

Innovations in consumption growth are driven by two independent shocks

$$\Delta c = \varepsilon + \eta, \quad (2.16)$$

where $\varepsilon \sim N(\mu, \sigma^2)$ and

$$\eta | (J = j) \sim N(j\theta, j\nu^2), \quad J \sim \mathbf{Poisson}(\kappa).$$

The interpretation of η is that of a jump component (disaster) which induces negative shocks to consumption growth. κ governs the jump intensity for the Poisson distribution. I use the same calibration as [Backus et al. \(2011\)](#). In line with their paper, the market return is considered as a claim on levered consumption, i.e. an asset that pays dividends C^λ . I convert the model implied volatility bounds to monthly units, to facilitate the comparison with the long-run risk model and the empirical bounds obtained in Section 3.2. The quantile bound, HJ bound and SDF volatility are illustrated in Panel (a) of Figure 2.⁹ We see that the quantile bound has a sharp peak at $\tau = 0.046$, after which it decreases monotonically. Interestingly, there is a range of τ values for which the quantile bound is sharper than the HJ bound.

This result can be understood from Panel (b) in Figure 2, which shows the physical and risk-neutral distribution of return on equity. The right tail of the distributions are not shown, since they are virtually indistinguishable in that region. The risk-neutral distribution displays a heavy left tail, owing to the implied disaster risk embedded in the SDF. As a result, it is extremely profitable to sell digital put options which pay out in case of a disaster. These put options must have high Sharpe ratios as their prices are high (insurance against disaster risk), but the actual probability of disaster is low enough that the risk associated to selling such insurance is limited.

The following example uses time t conditional information. I denote the SDF from time t to $t + 1$, by M_{t+1} . The subscript refers to a random variable that is realized at time $t + 1$, conditioned on time t .

Example 2.6 (Long-run risk). The long-run risk (LRR) model of [Bansal and Yaron \(2004\)](#) posits that consumption growth is driven by a small and persistent component that captures long-run risk. Moreover, the existence of a representative agent with [Epstein and Zin \(1989\)](#) recursive preferences is assumed. After calibration, this model is successful in matching many of the salient features of the US market return. I consider the extended model of [Bansal et al. \(2012\)](#), which allows for correlation between consumption growth shocks and dividend growth. In particular, the following

⁹The bounds can be calculated analytically, see Appendix A.5 for the details.

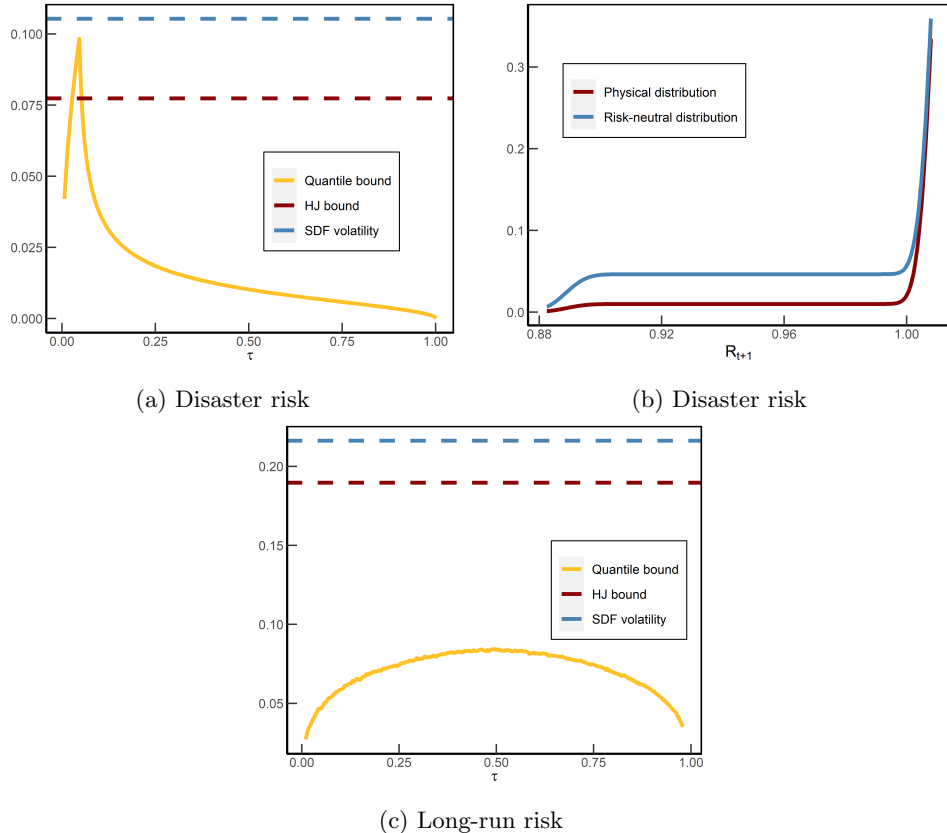


Figure 2: **Quantile and HJ bound for disaster risk and long-run risk model.** Panel (a) compares the quantile and HJ bound for the disaster risk model and Panel (b) shows the model implied physical and risk-neutral distribution. Panel (c) shows the quantile and HJ bound for the long-run risk model. The bounds and true SDF volatility are in monthly units.

dynamics are assumed:

$$\begin{aligned} x_{t+1} &= \rho x_t + \varphi_e \sigma_t e_{t+1} \\ \sigma_{t+1}^2 &= \bar{\sigma}^2 + \nu(\sigma_t^2 - \bar{\sigma}^2) + \sigma_w w_{t+1} \\ \Delta c_{t+1} &= \mu_c + x_t + \sigma_t \eta_{t+1} \\ \Delta d_{t+1} &= \mu_d + \phi x_t + \pi \sigma_t \eta_{t+1} + \varphi \sigma_t u_{d,t+1}. \end{aligned}$$

Here, Δc_{t+1} and Δd_{t+1} denote log consumption and dividend growth, while σ_t is the conditional volatility of log consumption growth. The parameter ρ governs the persistence of long-term risk. The log SDF dynamics follow from the Euler equation and the [Epstein and Zin \(1989\)](#) preferences

$$\log M_{t+1} = \theta \log \beta - \frac{\theta}{\psi} \Delta c_{t+1} + (\theta - 1) r_{c,t+1},$$

where $r_{c,t+1}$ is the continuous return on the consumption asset. I omit further details on the parameter interpretation and calibration approach, which is extensively discussed in [Bansal et al. \(2012\)](#). To compare the HJ bound to the quantile bound, I use the same calibration of parameters as [Bansal et al. \(2012\)](#). The quantile bound, as well as the HJ bound and SDF volatility are estimated by simulation, using 110,000 months, where the first 10,000 observations are dropped as burn-in sample. The results are summarized in Panel (c) of Figure 2. Unlike the disaster risk model, the quantile bound is always weaker than the HJ bound. Moreover, owing to the lognormal assumption, the quantile bound is almost symmetric around $\tau = 0.5$, at which the maximum is attained. Hence, it is not profitable to sell insurance against disaster risk, which contradicts the empirical results from Section 3.2.

3 Quantile bound in the data

3.1 Estimation of the unconditional quantile bound

In this section, I discuss the estimation of the quantile bound in (2.4) for monthly returns on the S&P 500 index. The quantile bound consists of three unknowns that need to be estimated: the physical distribution F , the risk-neutral quantile function \tilde{Q}_τ , and the risk-free rate R_f . I estimate the unconditional risk-free rate, denoted by \bar{R}_f , based on the average historical monthly interest rates. Let $R_{m,t+1}$ denote the monthly return on the S&P500 index from month t to $t + 1$. Since $R_{m,t+1}$ is drawn from the physical distribution, we can estimate F based on historical returns. In

particular, the estimator for F , denoted by \widehat{F} , is given by the kernel CDF estimator

$$\widehat{F} := \frac{1}{T} \sum_{t=1}^T \Phi \left(\frac{x - R_{m,t+1}}{h} \right), \quad (3.1)$$

where $\Phi(\cdot)$ is the Epanechnikov kernel and h is the bandwidth. I use a kernel CDF estimator, since a kernel ensures that the quantile bound is a smooth function of τ . Imposing a smooth quantile bound improves the approximation in finite samples and mitigates the influence of outliers that would be more pronounced if, say, we use the discontinuous empirical CDF estimator. The optimal bandwidth is determined via cross-validation.

Finally, I need to estimate the risk-neutral quantile function. To make this operational, I rely on the following result of [Breeden and Litzenberger \(1978\)](#):

$$\widetilde{F}_t \left(\frac{K}{S_t} \right) = R_{f,t} \frac{\partial}{\partial K} \text{Put}_t(K), \quad (3.2)$$

where \widetilde{F}_t is the time t conditional risk-neutral CDF of $R_{m,t+1}$, $R_{f,t}$ is the risk-free rate from month t to $t+1$, $\text{Put}_t(K)$ is the time t price of a European put option with strike K expiring at time $t+1$, and S_t is the time t price of the S&P500 index. Hence, with enough put option prices, we can identify the conditional risk-neutral distribution. I average the conditional distributions to estimate the unconditional CDF

$$\widehat{\widetilde{F}}(x) := \frac{1}{T} \sum_{t=1}^T \widetilde{F}_t(x).$$

Under suitable restrictions on the distribution of returns, we expect $\widehat{\widetilde{F}}$ to converge to the unconditional distribution as $T \rightarrow \infty$. An estimate for the unconditional risk-neutral quantile curve is then obtained from

$$\widehat{\widetilde{Q}}(\tau) := \inf \left\{ x \in \mathbb{R} : \tau \leq \widehat{\widetilde{F}}(x) \right\}. \quad (3.3)$$

It is a nontrivial exercise to obtain solid estimates via this procedure due to the lack of a continuum of option prices, interpolation of different maturity options and missing data for option prices far in- and out-of-the money. A detailed description of our approach that overcomes these issues is described in [Appendix B.2](#), which is based on [Filipović et al. \(2013\)](#).¹⁰

¹⁰This approach uses a kernel density and adds several correction terms to approximate the risk-neutral density. I follow [Barletta and Santucci de Magistris \(2018\)](#) and use a principal components step to avoid overfitting in the tails.

Based on the physical CDF (3.1) and risk-neutral quantile function (3.3), I estimate the quantile bound by

$$\widehat{\theta}(\tau) := \frac{|\tau - \widehat{\phi}(\tau)|}{\sqrt{\widehat{\phi}(\tau)(1 - \widehat{\phi}(\tau))\widehat{R}_f}}, \quad \tau \in [\varepsilon, 1 - \varepsilon] \subseteq (0, 1), \quad (3.4)$$

where $\widehat{\phi}(\tau) := \widehat{F}(\widehat{\tilde{Q}}(\tau))$ is the estimated ordinal dominance curve and ε is a small positive number.

3.2 Quantile bound for S&P500 returns

In this Section, I estimate the quantile bound for 30-day returns on the S&P500 index.¹¹ These returns are *non-overlapping* and sampled at the middle of each month over the period 1996-2021, which constitutes a total of 312 observations. I obtain the corresponding 30-day interest rates from Kenneth French's website.¹² The Sharpe ratio over this period is 13%, hence the HJ bound tells us that the (monthly) SDF is volatile. The historical returns are used to estimate the physical CDF in (3.1).

In order to estimate the risk-neutral quantile function in (3.3) for monthly returns, I need to use option prices. I use option data on the S&P500 index from OptionMetrics, sampled at the middle of each month, corresponding to the starting day of the returns.¹³ I use several data cleaning procedures to improve the estimation of the risk-neutral measure (see Appendix B.1). A detailed description of the estimation is given in Appendix B.2.

Panel (a) in Figure 3 shows the physical and risk-neutral CDF. In line with the disaster risk model in Panel (b) of Figure 2, we see that the physical and risk-neutral CDF differ most in the left tail. The quantile bound shows that this difference leads to a volatile SDF. The estimated quantile bound is shown in Panel (b) of Figure 3. The lower bound on the SDF volatility implied by the quantile bound is much stronger compared to the HJ bound in the left tail. This finding is consistent with empirical evidence which documents that high Sharpe ratios can be attained by selling out-of-the money put options (see Broadie et al. (2009) and the references therein). The quantile bound shows that high SDF volatility comes from the local difference between the physical and risk-neutral distribution around the 5th percentile. The non-monotonicity in the right tail of the quantile bound occurs because

¹¹I obtain these returns from WRDS.

¹²See http://mba.tuck.dartmouth.edu/pages/faculty/ken.french/data_library.html#Research

¹³Recall that $R_{m,t+1}$ denotes the S&P500 return from period t to $t+1$. Hence, the option prices are sampled on date t .

$\tilde{F}(x) > F(x)$, for x large enough. That is, the physical distribution does not first-order stochastically dominates the risk-neutral distribution.¹⁴

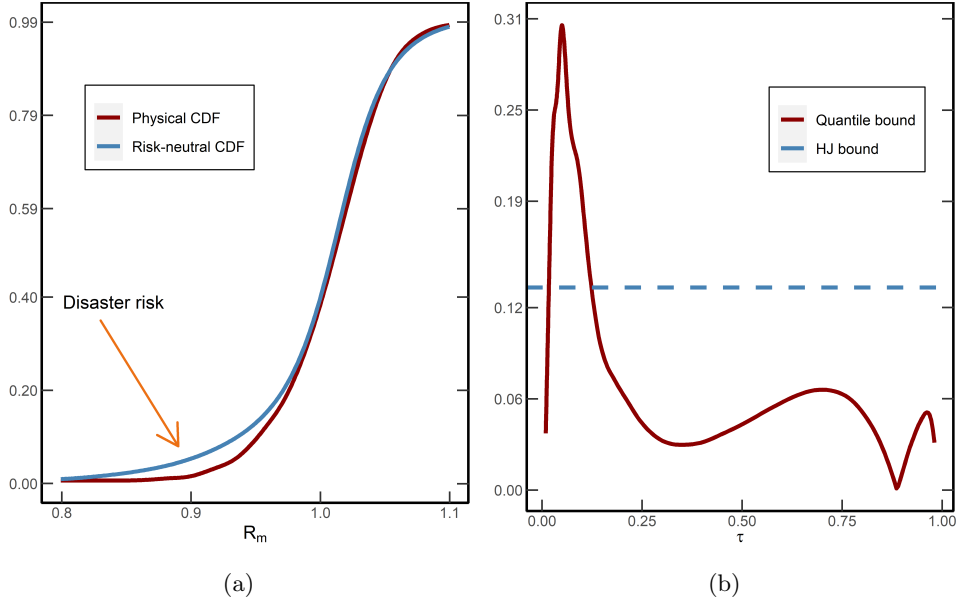


Figure 3: **Physical/risk-neutral CDF and quantile bound for monthly S&P500 returns.** Panel (a) shows the unconditional physical and risk-neutral CDF for monthly S&P500 returns, over the period 1996-2021. Panel (b) shows the quantile bound as function of τ , together with the HJ bound.

The graphical evidence suggests that the quantile bound renders a stronger bound on the SDF volatility than the HJ bound. To test this hypothesis more formally, I fix a priori the probability level at 0.046 ($\tau = 0.046$), which renders the sharpest bound on the SDF volatility in the disaster risk model (Example 2.5). At this probability level, the quantile bound is 30% in the data, which is more than twice as high as the HJ bound. To see whether this difference is statistically significant, I consider the following test statistic

$$\mathcal{T} := \hat{\theta}(0.046) - \frac{|\bar{R}_m - \bar{R}_f|}{\hat{\sigma}(R_m)\bar{R}_f}. \quad (3.5)$$

The first term on the right denotes the estimated quantile bound (3.4) evaluated at the 4.6th percentile, using the entire time series of returns $\{R_{m,t+1}\}$. The second term denotes the estimated HJ bound, using \bar{R}_m and $\hat{\sigma}(R_m)$ as the respective sample mean and standard deviation of $\{R_{m,t+1}\}$. A value of $\mathcal{T} > 0$ indicates that the quantile bound is stronger than the HJ bound. To test this restriction, I consider the null

¹⁴This result is consistent with Table 2, where I formally reject the null hypothesis that the physical distribution first-order stochastically dominates the risk-neutral distribution.

and alternative hypothesis:

$$\begin{aligned} H_0 : \mathcal{T} \leq 0 \\ H_1 : \mathcal{T} > 0. \end{aligned} \tag{3.6}$$

Since the distribution of (3.5) is hard to characterize, I use stationary bootstrap to approximate the p -value of the null hypothesis. The stationary bootstrap is used to generate time indices from which we recreate (with replacement) bootstrapped returns $\{R_{m,t+1}^*\}$ (Politis and Romano, 1994). The same bootstrapped time indices are used to re-estimate the physical CDF and risk-neutral quantile function. I repeat the bootstrap exercise 100,000 times and for each bootstrap sample, I calculate the test statistic \mathcal{T}^* . Finally, the empirical p -value is obtained as the fraction of times $\mathcal{T}^* \leq 0$. The last column in Table 1 shows that the p -value is 6%, which is at the borderline of rejecting H_0 .

However, many of the bootstrap samples do not contain disaster shocks when the HJ bound is stronger than the quantile bound. In fact, I find that the p -value is only 4% when I condition on bootstrap samples that include at least one month for which returns are less than -20%. There are only two returns in my sample that are less than -20%, namely on September 2008 and February 2020. I find that the p -value is 20% for bootstrap samples that do not include these months. These results underscore the sensitivity of the test to disaster shocks.

Table 1: **Sample bounds and bootstrap result**

Sample size	HJ bound	Quantile bound	p -value
312	0.13	0.30	0.06

Note: This table reports the HJ and quantile bound for monthly S&P500 returns over the period 1996–2021. The quantile bound is evaluated at $\tau = 0.0464$. The final column denotes the p -value of the null hypothesis in (3.6). The p -value is obtained from 100,000 bootstrap samples and counts the fraction of times that $\mathcal{T}^* \leq 0$.

3.3 Implications

In the previous Section, I showed that the quantile bound is stronger than the HJ bound. This observation presents a new challenge to asset pricing models. For example, in Section 2.3 I argued that any model which assumes joint normality between the SDF and return cannot generate a stronger quantile bound. The same is true for lognormal models under common calibration, as long as the time horizon is not too large. Intuitively, this follows since the tails of the physical and risk-neutral distribution are almost identical. However, in the data we find the opposite, namely that the left tails differ significantly (see Figure 3). The LRR model of Bansal et al. (2012)

can neither match a higher quantile bound, since the SDF and market return are lognormal. I establish by simulation that a risk aversion coefficient of 90 is needed for the quantile bound to overcome the HJ bound, which is beyond reasonable levels of risk aversion.

Also the shape of the quantile bound can be used to analyze misspecification. In particular, the empirical quantile bound is highly asymmetric and in the right tail, the bound is significantly weaker than the HJ bound. The disaster risk model predicts the exact same behavior, since shocks to the market are assumed to be negative conditional on a jump. This assumption implies that the physical and risk-neutral distribution only differ much in the left tail, which creates an asymmetry in the quantile bound. In contrast, the lognormal assumption implies that the quantile bound is almost symmetric and that the physical and risk-neutral distribution differ most around the median. The empirical results thus reveal the importance of embedding disaster risk in an asset pricing model. A local analysis based on the quantile bound is crucial to uncover this stylized fact. This local analysis is what distinguishes my approach from the misspecification literature, which is typically based on global bounds such as variance or other higher order moments.

4 Conditional relation between physical and risk-neutral quantile

The unconditional quantile bound puts a tight constraint on the SDF volatility due to the local difference between the physical and risk-neutral distribution in the left tail. This section complements that finding by incorporating conditional information. I use QR to show that the physical and risk-neutral distribution continue to differ most in the left tail conditional on time t . Subsequently, I derive a risk-adjustment term that shifts the risk-neutral quantile closer to the physical quantile in the left tail. This risk-adjustment term, which is nonparametric, renders a model-free measure of disaster risk.

4.1 Notation and data

In my application, the length of the return period is either 30, 60 or 90 days. I use *overlapping returns* and denote these by $R_{m,t \rightarrow N}$, where the subscript signifies the return between period t and $t + N$. I denote the risk-free rate over the same period by $R_{f,t \rightarrow N}$, which is assumed to be known at time t . Throughout this Section,

$F_t(x) := \mathbb{P}(R_{m,t \rightarrow N} \leq x | \mathcal{F}_t)$ denotes the physical CDF of the market return conditional on all information \mathcal{F}_t available at time t , $f_t(\cdot)$ denotes the conditional PDF and $Q_{t,\tau}$ denotes the conditional τ -quantile. As before, a tilde superscript refers to the risk-neutral measure. Notice that the risk-neutral distribution and realized return are both conditional on the same information set \mathcal{F}_t . The conditional risk-neutral quantile function can be estimated nonparametrically at time t using (3.2), but the physical measure cannot be estimated since we observe only a single draw from that distribution.

As in Section 3.2, I use returns on the S&P500 index as a proxy for the market return. I use put and call option prices on each day t to estimate the risk-neutral quantile function $\tilde{Q}_{t,\tau}$, following the procedure in Appendix B.1. I discard all observations prior to 2003, since there are many days in the period 1996-2003 that have insufficient option data to estimate $\tilde{Q}_{t,\tau}$. Occasionally it happens that I cannot estimate the risk-neutral quantile on a specific day in the post 2003 period and I discard these days as well.¹⁵ In total, I'm left with 4333, 4312 and 4291 daily observations for the respective 30, 60 and 90 day horizons over the period 2003-2021.

4.2 Risk-neutral quantile regression

In reduced form, the disaster risk literature (Barro, 2006; Backus et al., 2011; Gabaix, 2012; Wachter, 2013) makes the assumption that shocks to the market return are negative conditional on a disaster. This assumption implies the fat left tail in the risk-neutral distribution shown in Panel (a) of Figure 2, but the right tail of the risk-neutral and physical distribution are nearly identical. In contrast, the LRR model implies that the risk-neutral and physical distribution differ most around the median due to the conditional lognormal assumption. In order to understand which part of the physical distribution is most subject to risk-adjustment conditional on \mathcal{F}_t , I use quantile regression (Koenker and Bassett, 1978).

Suppose momentarily that the physical quantile is given by

$$Q_{t,\tau}(R_{m,t \rightarrow N}) = \beta_0(\tau) + \beta_1(\tau)\tilde{Q}_{t,\tau}, \text{ for all } \tau \in (0, 1). \quad (4.1)$$

Given a sample of T observations $\{R_{m,t \rightarrow N}, \tilde{Q}_{t,\tau}\}_{t=1}^T$, we can estimate the unknown parameters by

$$[\hat{\beta}_0(\tau), \hat{\beta}_1(\tau)] = \arg \min_{\beta_0, \beta_1 \in \mathbb{R}} \sum_{t=1}^T \rho_\tau(R_{m,t \rightarrow N} - \beta_0 - \beta_1 \tilde{Q}_{t,\tau}), \quad (4.2)$$

¹⁵The number of days I cannot estimate the risk-neutral PDF is very small, about 2% in total. Most of these days occur at the beginning of the sample period.

where $\rho_\tau(x) = x(\tau - \mathbb{1}(x < 0))$ is the check function from quantile regression (QR). Even if (4.1) is misspecified, Angrist et al. (2006) show that QR finds the best linear approximation to the conditional quantile function. This result is analogous to OLS, which finds the best linear approximation to the conditional *expectation* function, even if the model is misspecified.

If the world is risk-neutral, $Q_{t,\tau}(R_{m,t \rightarrow N}) = \tilde{Q}_{t,\tau}$ and $[\hat{\beta}_0(\tau), \hat{\beta}_1(\tau)] \rightarrow [0, 1]$ in probability. More generally, the disaster risk models predict $[\beta_0(\tau), \beta_1(\tau)] \approx [0, 1]$ for all $\tau > \kappa > 0.5$, for some κ far enough in the right tail. QR allows me to assess these different hypotheses by testing how close $[\beta_0(\tau), \beta_1(\tau)]$ is to the $[0, 1]$ benchmark for different τ . The setup in (4.1) is nonstandard since the regressor changes with τ , unlike most quantile regressions where the independent variable is fixed across τ . Notice also that (4.1) properly accounts for conditional information since $R_{m,t \rightarrow N}$ and $\tilde{Q}_{t,\tau}$ belong to the same information set \mathcal{F}_t .

Table 2 shows the QR estimates in (4.2). The null hypothesis that $[\beta_0(\tau), \beta_1(\tau)] = [0, 1]$ is (borderline) rejected for all $\tau \leq 0.2$, at all horizons. In contrast, the null hypothesis is never rejected for $\tau \geq 0.8$ and the point estimates are close to $[0, 1]$ at all horizons. These results suggest that the physical and risk-neutral distribution locally differ most in the left tail conditional on time t , exactly as the disaster risk models predict. The standard errors in Table 2 are obtained by the smooth extended tapered block bootstrap (SETBB) of Gregory et al. (2018), which is robust to heteroscedasticity and weak dependence. This robustness is important in the estimation, since I use overlapping returns which creates time dependence in the error term, akin to the overlapping observation problem in OLS (Hansen and Hodrick, 1980). SETBB also renders an estimate of the covariance matrix between $\hat{\beta}_0(\tau)$ and $\hat{\beta}_1(\tau)$, which can be used to test joint restrictions on the coefficients.¹⁶

Table 2 contains two other measures of fit that can be used gauge how well the risk-neutral distribution approximates the physical distribution. The first measure, $R^1(\tau)$, is defined as¹⁷

$$R^1(\tau) := 1 - \frac{\min_{b_0, b_1} \sum_{t=1}^T \rho_\tau(R_{m,t \rightarrow N} - b_0 - b_1 \tilde{Q}_{t,\tau})}{\min_{b_0} \sum_{t=1}^T \rho_\tau(R_{m,t \rightarrow N} - b_0)}. \quad (4.3)$$

This measure of fit was proposed by Koenker and Machado (1999) and is a clean substitute for the OLS R^2 . Table 2 shows that the in-sample fit in the right tail is

¹⁶I use the `QregBB` function from the *R* package `QregBB`, available on the author's Github page: <https://rdrr.io/github/gregorkb/QregBB/man/QregBB.html>. The only user required input for this method is the block length in the bootstrap procedure.

¹⁷It is well known that b_0 in the denominator of (4.3) equals the in-sample τ -quantile.

much better compared to the left tail according to $R^1(\tau)$. Second, to measure the out-of-sample fit, I use

$$R_{oos}^1(\tau) := 1 - \frac{\sum_{t=w}^T \rho_\tau(R_{m,t \rightarrow N} - \tilde{Q}_{t,\tau})}{\sum_{t=w}^T \rho_\tau(R_{m,t \rightarrow N} - \bar{Q}_{t,\tau})}, \quad (4.4)$$

where w is the rolling window length and $\bar{Q}_{t,\tau}$ is the *historical rolling quantile* of the market return from time $t - w + 1$ to t . $R_{oos}^1(\tau)$ is a natural analogue of the out-of-sample R^2 proposed by [Campbell and Thompson \(2008\)](#) in the context of conditional mean regression. Notice that (4.4) is a genuine out-of-sample metric, since no parameter estimation is used. Table 2 shows that, out-of-sample, the risk-neutral quantile fares better in the right tail than the left tail. Hence, the risk-neutral distribution approximates the physical distribution much better in the right tail, both in- and out-of-sample. Investors in the market return thus get compensated for bearing downside risk, but not upside risk.

The implications of Table 2 are quite rich and other asset pricing puzzles, such as monotonicity of the pricing kernel naturally emerge using the combination of realized returns and risk-neutral quantiles. Table 2 reports the expected value of the hit function, defined as

$$\text{Hit}_t = \mathbb{1}(R_{m,t \rightarrow N} < \tilde{Q}_{t,\tau}) - \tau. \quad (4.5)$$

The expected value of Hit_t yields another measure of the difference between F_t and \tilde{F}_t . In particular, the expected value is 0 if investors are risk-neutral. It turns out that (4.5) is negative for all τ if the pricing kernel is a monotonic function of $R_{m,t \rightarrow N}$.¹⁸ In contradiction to monotonicity, Table 2 shows that the sample expectation of Hit_t is positive for $\tau = 0.95$, at the 30 and 60 day horizon. I find, using stationary bootstrap, that the estimated expectation is significantly different from zero. This result is consistent with a *U*-shaped pricing kernel ([Aït-Sahalia and Lo, 1998](#); [Jackwerth, 2000](#); [Rosenberg and Engle, 2002](#); [Bakshi et al., 2010](#)). In addition, my approach is not subject to the conditioning critique of [Linn et al. \(2018\)](#), since the estimation relies on the empirical mean of $\mathbb{1}(R_{m,t \rightarrow N} \leq \tilde{Q}_{t,\tau})$, and $\{\tilde{Q}_{t,\tau}, R_{m,t \rightarrow N}\}$ belong to the same conditional information set.

Finally, Table 2 also connects to the recovery of beliefs ([Ross, 2015](#); [Borovička et al., 2016](#)). Namely, the right tail of the physical distribution can be accurately recovered from the right tail of the risk-neutral distribution, which is observed con-

¹⁸To see this, we can directly apply the arguments of [Beare and Schmidt \(2016\)](#), who show that monotonicity is equivalent to the ordinal dominance curve being concave (or convex, since we defined the ordinal dominance curve as $\phi(\tau) = F(\tilde{F}^{-1}(\tau))$).

ditional on time t . Hence, there is a specific part of the return distribution that can be recovered from option prices. In the next Section, I outline how we can approximately recover the left tail of the physical distribution.

Table 2: **Risk-neutral quantile regression**

Horizon	τ	$\hat{\beta}_0(\tau)$	$\hat{\beta}_1(\tau)$	Wald test	Hit[%]	$R^1(\tau)[\%]$	$R_{oos}^1(\tau)[\%]$
30 days*	0.05	0.43 (0.225)	0.56 (0.240)	0.01	-2.67	6.28	6.11
	0.1	0.45 (0.241)	0.54 (0.251)	0.03	-3.56	3.45	1.01
	0.2	0.69 (0.399)	0.30 (0.407)	0.11	-3.73	0.55	0.89
	0.5	-0.60 (0.307)	1.61 (0.305)	0	-8.07	1.65	2.24
	0.8	-0.09 (0.160)	1.09 (0.156)	0.2	-3.24	12.44	12.5
	0.9	0.03 (0.123)	0.97 (0.118)	0.97	-0.04	20.41	21.88
	*(Obs. 4333)	0.95	0.12 (0.122)	0.89 (0.116)	0.51	0.27	31.31
60 days**	0.05	0.45 (0.323)	0.54 (0.367)	0.01	-3.33	3.12	13.14
	0.1	0.58 (0.324)	0.41 (0.348)	0.02	-5.57	1.79	3.5
	0.2	0.78 (0.424)	0.21 (0.436)	0.05	-6.6	0.38	-0.03
	0.5	-1.02 (0.426)	2.01 (0.421)	0.02	-7.88	2.81	3.86
	0.8	-0.08 (0.209)	1.08 (0.120)	0.11	-5.53	12.7	12.23
	0.9	0.04 (0.149)	0.96 (0.141)	0.57	-1.94	21.66	22.79
	**(Obs. 4312)	0.95	0.04 (0.130)	0.96 (0.121)	0.91	0.43	34.19
90 days***	0.05	0.60 (0.438)	0.37 (0.518)	0.02	-2.95	2.9	15.63
	0.1	0.59 (0.412)	0.40 (0.456)	0	-6.36	3.46	3.84
	0.2	0.57 (0.593)	0.43 (0.613)	0.09	-7.53	0.83	1.93
	0.5	-0.99 (0.653)	1.99 (0.641)	0.03	-10.85	2.58	0.18
	0.8	-0.23 (0.258)	1.23 (0.244)	0.32	-6.66	15.47	16.54
	0.9	-0.02 (0.184)	1.02 (0.170)	0.86	-1.12	23.18	27.92
	***(Obs. 4291)	0.95	0.08 (0.158)	0.93 (0.144)	0.87	-0.06	39.88

Note: This table reports the QR estimates of (4.2) over the sample period 2003–2021 at different horizons, using overlapping returns. Standard errors are shown in parentheses and based on SETBB with a block length of 5 times the prediction horizon. Hit refers to the sample expectation of (4.5). $R^1(\tau)$ denotes the goodness of fit measure (4.3). $R_{oos}^1(\tau)$ is the out-of-sample goodness of fit (4.24) (based on $\hat{Q}_{t,\tau}$), using a rolling window of size 10 times the prediction horizon.

4.3 Lower bound on physical quantile

The risk-neutral quantile is not a good approximation to the physical quantile function in the left tail. I now derive a risk-adjustment term that better approximates $Q_{t,\tau}$. The latent quantile function $Q_{t,\tau}$ in the left tail is of direct interest, since it gives a measure of *conditional disaster risk*.

I use the differentiable calculus for statistical functionals to approximate the difference between $Q_{t,\tau}$ and $\tilde{Q}_{t,\tau}$ in the left tail. The quantile function can be regarded as a map φ between normed spaces, taking as input a distribution function and returning the quantile function. In mathematical notation, $\varphi(F_t) = F_t^{-1} = Q_{t,\tau}$. I expand φ around the observed risk-neutral CDF to obtain

$$Q_{t,\tau} - \tilde{Q}_{t,\tau} = \varphi(F_t) - \varphi(\tilde{F}_t) = \varphi'_{\tilde{F}_t}(F_t - \tilde{F}_t) + o\left(\|F_t - \tilde{F}_t\|\right), \quad (4.6)$$

where $\|\cdot\|$ is a norm on a suitable linear space¹⁹ and $\varphi'_{\tilde{F}_t}(F_t - \tilde{F}_t)$ is the Gâteaux derivative of φ at \tilde{F}_t in the direction of F_t :

$$\begin{aligned} \varphi'_{\tilde{F}_t}(F_t - \tilde{F}_t) &:= \lim_{\lambda \downarrow 0} \frac{\varphi\left[(1 - \lambda)\tilde{F}_t + \lambda F_t\right]}{\lambda} \\ &= \frac{\partial}{\partial \lambda} \varphi\left((1 - \lambda)\tilde{F}_t + \lambda F_t\right) \Big|_{\lambda=0}. \end{aligned} \quad (4.7)$$

Heuristically, the Gâteaux derivative can be thought of as measuring the change in the quantile function when we move the risk-neutral distribution in the direction of the physical distribution. Appendix A.8 shows that the Gâteaux derivative is given by

$$\varphi'_{\tilde{F}_t}(F_t - \tilde{F}_t) = \frac{\tau - F_t(\tilde{Q}_{t,\tau})}{\tilde{f}_t(\tilde{Q}_{t,\tau})}. \quad (4.8)$$

I proceed under the working hypothesis that the remainder term in (4.6) is “small” in the sup-norm, $\|g\|_\infty = \sup_x |g(x)|$.

Assumption 4.1. *The remainder term in (4.6) can be neglected.*

Remark. I simply assume that the first order approximation in (4.6) is accurate. The assumption that $\|F_t - \tilde{F}_t\|_\infty$ is small can be understood as excluding near-arbitrage opportunities, since the discussion in Example 2.5 shows that substantial pointwise difference between $F_t(\cdot)$ and $\tilde{F}_t(\cdot)$ leads to a very volatile SDF. Ultimately, whether Assumption 4.1 is reasonable or not is an empirical question. In Section 4.4, I provide

¹⁹Formally, the space can be defined as $\{\Delta : \Delta = c(F - G), F, G \in \mathbb{D}, c \in \mathbb{R}\}$ and \mathbb{D} is the space of distribution functions (Serfling, 2009). See van der Vaart (2000, Section 20.1) and Serfling (2009, p. 217) for further details about the approximation.

empirical support that the approximation is quite accurate. Additionally, Appendix E.3 shows that Assumption 4.1 finds support in the [Black and Scholes \(1973\)](#) model.

I combine (4.6) and (4.8) in conjunction with Assumption 4.1 to obtain the approximation

$$Q_{t,\tau} \approx \tilde{Q}_{t,\tau} + \underbrace{\frac{\tau - F_t(\tilde{Q}_{t,\tau})}{\tilde{f}_t(\tilde{Q}_{t,\tau})}}_{\text{risk-adjustment}}. \quad (4.9)$$

Observe that the numerator in the risk adjustment term equals the numerator term in the conditional version of the quantile bound. The approximation in (4.9) contains the terms $\tilde{Q}_{t,\tau}$ and $\tilde{f}_t(\tilde{Q}_{t,\tau})$, which are directly observed at time t as they can be estimated using (a variation of) the [Breeden and Litzenberger \(1978\)](#) formula in (3.2). However, the physical CDF is unknown and hence (4.9) cannot be used directly to measure $Q_{t,\tau}$.

To make further progress, I show that the numerator term, $\tau - F_t(\tilde{Q}_{t,\tau})$, can be bounded with option data under certain economic constraints. [Chabi-Yo and Loudis \(2020\)](#) show that in representative agent models, the SDF is a function of the market return:

$$\frac{\mathbb{E}_t[M_{t \rightarrow N}]}{M_{t \rightarrow N}} = \frac{\frac{u'(W_t x_0)}{u'(W_t x)}}{\tilde{\mathbb{E}}_t\left[\frac{u'(W_t x_0)}{u'(W_t x)}\right]} \quad \text{with } x = R_{m,t \rightarrow N} \text{ and } x_0 = R_{f,t \rightarrow N}, \quad (4.10)$$

where W_t is the agent's wealth at time t and $u(x)$ is the utility function. Define

$$\zeta(x) := \frac{u'(W_t R_{f,t \rightarrow N})}{u'(W_t x)} \quad \text{and} \quad \theta_k = \frac{1}{k!} \left(\frac{\partial^k \zeta(x)}{\partial x^k} \right)_{x=R_{f,t \rightarrow N}}. \quad (4.11)$$

I make the following assumptions about the market return and the utility function of the representative agent.

Assumption 4.2. (i) $\tilde{\mathbb{E}}_t[R_{m,t \rightarrow N}^4] < \infty$. (ii) $\zeta^{(4)}(x) \leq 0$. (iii) The marginal rate of substitution satisfies

$$\int_0^1 \zeta^{(4)}(R_{f,t \rightarrow N}(1-s)) (1-s)^3 ds < \tilde{\mathbb{E}}_t[G(R_{m,t \rightarrow N})] \quad \text{or} \quad \zeta^{(4)}(x) = 0, \quad (4.12)$$

where

$$G(x) = \frac{(x - R_{f,t \rightarrow N})^4}{4!} \int_0^1 \zeta^{(4)}(R_{f,t \rightarrow N} + s(x - R_{f,t \rightarrow N})) (1-s)^3 ds.$$

Part (i) allows for fat tails in the risk-neutral distribution as long as the kurtosis is finite. [Chabi-Yo and Loudis \(2020\)](#) present sufficient conditions for part (ii) to hold,

which relate to the sign of the n th derivative of the utility function in the expected utility framework. Part (iii) is sufficient to establish the lower bound in Theorem 4.3. I show that (iii) holds for some common utility functions in Section A.7.1. The second condition in (4.12) is needed to deal with special cases such as log utility.

Under Assumption 4.2, we can bound the difference between the physical and risk-neutral distribution.

Theorem 4.3 (Infeasible lower bound). *Let Assumption 4.2 hold and assume that the risk-neutral CDF is absolutely continuous with respect to Lebesgue measure. Define τ^* so that $G(\tilde{Q}_{t,\tau^*}) = G(R_{m,t \rightarrow N})$. Then for all $\tau \leq \tau^*$,*

$$\tau - F_t(\tilde{Q}_{t,\tau}) \geq \frac{\sum_{k=1}^3 \theta_k (\tau \tilde{\mathbb{M}}_{t \rightarrow N}^{(k)} - \tilde{\mathbb{M}}_{t \rightarrow N}^{(k)}[\tilde{Q}_{t,\tau}])}{1 + \sum_{k=1}^3 \theta_k \tilde{\mathbb{M}}_{t \rightarrow N}^{(k)}}, \quad (4.13)$$

where

$$\begin{aligned} \tilde{\mathbb{M}}_{t \rightarrow N}^{(n)} &:= \tilde{\mathbb{E}}_t [(R_{m,t \rightarrow N} - R_{f,t \rightarrow N})^n] \\ \tilde{\mathbb{M}}_{t \rightarrow N}^{(n)}[k_0] &:= \tilde{\mathbb{E}}_t [\mathbb{1}(R_{m,t \rightarrow N} \leq k_0) (R_{m,t \rightarrow N} - R_{f,t \rightarrow N})^n]. \end{aligned} \quad (4.14)$$

Proof. See Appendix A.7. ■

The (un)truncated moments in (4.14) can be computed from option prices (see Appendix A.6), but the bound in (4.13) is still infeasible since θ_k is unknown.²⁰ However, Chabi-Yo and Loudis (2020, Table 6) provide empirical evidence that

$$\theta_1 = \frac{1}{R_{f,t \rightarrow N}}, \theta_2 = -\frac{1}{R_{f,t \rightarrow N}^2}, \text{ and } \theta_3 = \frac{1}{R_{f,t \rightarrow N}^3}. \quad (4.15)$$

Under (4.15), I can obtain a feasible bound on $\tau - F_t(\tilde{Q}_{t,\tau})$.

Corollary 4.4 (Feasible lower bound). *Suppose the assumptions of Theorem 4.3 hold. In addition, suppose that (4.15) holds. Then for all $\tau \leq \tau^*$,*

$$\tau - F_t(\tilde{Q}_{t,\tau}) \geq \frac{\sum_{k=1}^3 \frac{(-1)^{k+1}}{R_{f,t \rightarrow N}^k} (\tau \tilde{\mathbb{M}}_{t \rightarrow N}^{(k)} - \tilde{\mathbb{M}}_{t \rightarrow N}^{(k)}[\tilde{Q}_{t,\tau}])}{1 + \sum_{k=1}^3 \frac{(-1)^{k+1}}{R_{f,t \rightarrow N}^k} \tilde{\mathbb{M}}_{t \rightarrow N}^{(k)}} =: \text{LB}_{t,\tau}. \quad (4.16)$$

Proof. See Appendix A.7. ■

Under the working hypothesis that the remainder term in the quantile approximation in (4.9) is negligible, the following Corollary is immediate.

²⁰In Appendix C, I provide closed form expressions of (A.17) for commonly used utility functions. These expressions generalize the equity premium results of Martin (2017) and Chabi-Yo and Loudis (2020) to the whole distribution.

Corollary 4.5. *Under the same assumptions of Corollary 4.4 and assuming that the remainder term in (4.9) is negligible, we have*

$$Q_{t,\tau} - \tilde{Q}_{t,\tau} \geq \underbrace{\frac{\text{LB}_{t,\tau}}{\tilde{f}_t(\tilde{Q}_{t,\tau})}}_{\text{risk-adjustment}} =: \text{RA}_{t,\tau}. \quad (4.17)$$

The bound in Corollary 4.4 does not require any parameter estimation and can be calculated solely based on time t information. Corollary 4.4 complements the recent literature on the recovery of beliefs. [Ross \(2015\)](#) shows that one can recover F_t , if the pricing kernel is transition independent. Subsequent work ([Borovička et al., 2016](#); [Qin et al., 2018](#); [Jackwerth and Menner, 2020](#)) casts doubt on the transition independence assumption and shows that recovery is generally impossible. Complimentary to these results, Corollary 4.4 shows that one can still establish a lower bound on the left tail of the physical distribution, using a different set of (mild) economic constraints. Moreover, I showed in Section 4.2 that the right tail of F_t can be recovered from the risk-neutral distribution due to the near absence of risk-adjustment. Both results combined show that approximate recovery of F_t using option prices is still possible.

Corollary 4.5 establishes a lower bound on the difference between the physical and risk-neutral quantile function, which can be thought of as a risk-adjustment term. If the lower bound in (4.17) happens to be tight, it gives us a direct measure of conditional disaster risk. In addition, the term on the right of (4.17) is not subject to the historical sample bias critique of [Welch and Goyal \(2008\)](#) and it is available at a daily frequency. The motivation for introducing disaster risk is to explain the historically high equity premium ([Rietz, 1988](#); [Barro, 2006](#)). However, a high (conditional) equity premium does not necessarily arise due to disaster risk and, moreover, calibrating these models is difficult due to the lack of disasters in the data ([Martin, 2013](#)). For these reasons, it is of interest to approximate $Q_{t,\tau}$ in the left tail using a model-free approach. In the next Section, I show that the assumption of a tight lower bound in (4.17) cannot be rejected.

4.4 How tight is the lower bound in Corollary 4.5?

4.4.1 Estimation of the lower bound

I first outline the procedure to calculate $\text{LB}_{t,\tau}$ and $\tilde{f}_t(\tilde{Q}_{t,\tau})$, which are needed to compute the lower bound in Corollary 4.5. Since $\frac{d}{d\tau} \tilde{Q}_t(\tau) = 1/\tilde{f}_t(\tilde{Q}_{t,\tau})$, I approximate

the denominator term in (4.17) by

$$\frac{1}{\tilde{f}_t(\tilde{Q}_{t,\tau})} \approx \frac{\tilde{Q}_t(\tau+h) - \tilde{Q}_t(\tau-h)}{2h},$$

where h is the bandwidth of the τ -grid. Second, to calculate $\text{LB}_{t,\tau}$ from (4.16), I use the estimated quantile curve $\tilde{Q}_{t,\tau}$ in combination with the formula for higher order risk-neutral moments in Appendix A.6.

Since virtually all macro-finance models assume that the market return is negatively correlated with the SDF, one expects the market return to have a higher probability of a crash under risk-neutral measure than under physical measure. This means that Corollary 4.5 has non trivial content if $\text{LB}_{t,\tau} \geq 0$ in the data. I confirm that $\text{LB}_{t,\tau} \geq 0$ for all dates considered, using the same τ 's from Table 4 below. Appendix Table E1 contains summary statistics of $\text{RA}_{t,\tau}$, which show that the risk-adjustment term is right-skewed, more pronounced in the right tail and economically meaningful in magnitude, with outliers that can spike up to 29%.

4.4.2 In-sample performance

To test whether the lower bound in Corollary 4.5 is tight, I form *excess quantile returns*, $R_{m,t \rightarrow N} - \tilde{Q}_{t,\tau}$. Since $\tilde{Q}_{t,\tau}$ is observed at time t , we have $Q_{t,\tau}(R_{m,t \rightarrow N} - \tilde{Q}_{t,\tau}) = Q_{t,\tau}(R_{m,t \rightarrow N}) - \tilde{Q}_{t,\tau}$. Subsequently, I use QR to estimate the model

$$\begin{aligned} Q_{t,\tau}(R_{m,t \rightarrow N}) - \tilde{Q}_{t,\tau}(R_{m,t \rightarrow N}) &= \beta_0(\tau) + \beta_1(\tau)\text{RA}_{t,\tau}, \\ [\hat{\beta}_0(\tau), \hat{\beta}_1(\tau)] &= \arg \min_{\beta_0, \beta_1 \in \mathbb{R}} \sum_{t=1}^T \rho_\tau(R_{m,t \rightarrow N} - \tilde{Q}_{t,\tau} - \beta_0 - \beta_1 \text{RA}_{t,\tau}). \end{aligned} \quad (4.18)$$

Regression (4.18) is similar in spirit to the excess return regressions of [Welch and Goyal \(2008\)](#). Under the null hypothesis that the lower bound is tight, we have

$$H_0 : [\beta_0(\tau), \beta_1(\tau)] = [0, 1]. \quad (4.19)$$

Less restrictive, we can test whether $\beta_0(\tau) = 0$ and $\beta_1(\tau) > 0$, which implies that the statistical “factor” $\text{RA}_{t,\tau}$ explains the conditional quantile wedge.²¹

Table 3 shows the result of regression (4.18). The null hypothesis of a tight lower bound in (4.19) cannot be rejected for $\tau = 0.2$, but is rejected for $\tau \in \{0.05, 0.1\}$

²¹For example, if we start with a quantile factor model $Q_{t,\tau} = \tilde{Q}_{t,\tau} + \beta(\tau)\text{RA}_{t,\tau}$, the model has one testable implication for the data: the intercept in a quantile regression of $R_{m,t \rightarrow N} - \tilde{Q}_{t,\tau}$ on $\text{RA}_{t,\tau}$ should be zero. Quantile factor models have recently been proposed by [Chen et al. \(2021\)](#).

at all horizons. In case the null hypothesis is rejected, the $\beta_1(\tau)$ -coefficient is larger than 1, which is consistent with the theory that $\text{RA}_{t,\tau}$ represents a lower bound on the difference between the physical and risk-neutral distribution. Table 3 also documents p -values of the joint hypothesis in (4.19), which again is not rejected for $\tau = 0.2$ only. In all cases, the lower bound is economically meaningful since $\beta_1(\tau)$ is significantly different from 0, while $\beta_0(\tau) = 0$ can never be rejected. To shed more light on the explanatory power of the lower bound, I use the $R^1(\tau)$ analogue of (4.3)

$$R^1(\tau) = 1 - \frac{\min_{b_0, b_1} \sum \rho_\tau(R_{m,t \rightarrow N} - b_0 - b_1 \text{RA}_{t,\tau})}{\min_{b_0} \sum \rho_\tau(R_{m,t \rightarrow N} - b_0)}. \quad (4.20)$$

Table 3 shows that the explanatory power of $\text{RA}_{t,\tau}$ is modest, generally around a few percent. Low explanatory power is typical in the equity premium literature, since high R^2 -values lead to high Sharpe ratios, as market timing strategies can be designed to exploit return predictability (Ross, 2005; Campbell and Thompson, 2008). The same logic applies in the quantile case, since the quantile bound in Theorem 2.1 shows that large pointwise differences between the physical and risk-neutral distribution lead to near arbitrage opportunities. If one could predict this difference, one could again design a trading strategy that exploits the predictability, this time using options rather than a direct timing investment in the market portfolio.

Another way to test whether the lower bound in 4.5 represents a meaningful risk-adjustment term is to test directly whether the following is a good proxy for the latent conditional quantile function

$$\hat{Q}_{t,\tau} = \tilde{Q}_{t,\tau} + \text{RA}_{t,\tau}. \quad (4.21)$$

I use QR to estimate the model

$$Q_{t,\tau}(R_{m,t \rightarrow N}) = \beta_0(\tau) + \beta_1(\tau) \hat{Q}_{t,\tau}. \quad (4.22)$$

If (4.21) is a good predictor of the conditional quantile function, we have under the null hypothesis

$$H_0 : \beta_0(\tau) = 0, \quad \beta_1(\tau) = 1. \quad (4.23)$$

Table 4 summarizes the estimates of (4.22) for several quantiles. The results uniformly improve upon the risk-neutral estimates in Table 2. First, the point estimates for $[\beta_0(\tau), \beta_1(\tau)]$ are closer to the $[0, 1]$ benchmark. Second, the Wald test on the joint restriction in (4.23) is never rejected and third, the in-sample explanatory power is higher. These results suggest that $\hat{Q}_{t,\tau}$ can be regarded as a good proxy for the latent conditional quantile function $Q_{t,\tau}$.

Table 3: **Quantile regression lower bound**

	Horizon	$\hat{\beta}_0(\tau)$	$\hat{\beta}_1(\tau)$	Wald test	$R^1(\tau)[\%]$	Obs
$\tau = 0.05$	30 days	-0.01 (0.006)	4.43 (0.357)	0	6.03	4333
	60 days	-0.01 (0.018)	5.53 (0.681)	0	3.6	4312
	90 days	-0.02 (0.040)	6.37 (1.364)	0	4.91	4291
$\tau = 0.1$	30 days	-0.01 (0.005)	2.17 (0.408)	0.02	3.18	4333
	60 days	-0.02 (0.016)	3.25 (0.668)	0	2.23	4312
	90 days	-0.02 (0.024)	3.05 (0.688)	0	4.43	4291
$\tau = 0.2$	30 days	-0.01 (0.006)	1.33 (0.412)	0.03	0.41	4333
	60 days	-0.02 (0.012)	1.50 (0.484)	0.47	0.48	4312
	90 days	-0.02 (0.022)	1.36 (0.704)	0.77	1.46	4291

Note: This table reports the QR estimates of (4.18) over the sample period 2003-2021 at different horizons, using overlapping returns. Standard errors are shown in parentheses and calculated using SETBB with a block length of maturity times 5. Wald test denotes the p -value of the joint restriction $[\beta_0(\tau), \beta_1(\tau)] = [0, 1]$. $R^1(\tau)$ denotes the goodness-of-fit measure (4.20).

Two additional remarks are in order. First, since we estimate $\hat{Q}_{t,\tau}$ from option prices, there might be a concern for attenuation bias due to measurement error (Angrist et al., 2006). In Appendix E.4, I provide simulation evidence which shows that attenuation bias is negligible in a setup that mimics the empirical application. Second, there is a possibility of quantile crossing, which means that the predicted quantiles, $\hat{\beta}_0(\tau) + \hat{\beta}_1(\tau)\text{RA}_{t,\tau}$, are not monotone with respect to τ . This problem frequently arises in dynamic quantile models (Gouriéroux and Jasiak, 2008). It appears however, not a concern in our case, since crossing occurs only 0.04% of the time for the 30 day horizon. For the other horizons, crossing happens about 0.1% of the time; again a very small amount of the total number of return observations.²²

4.4.3 Out-of-sample performance

Since the in-sample results for the physical quantile approximation suggest $\beta_0(\tau) = 0$ and $\beta_1(\tau) = 1$, it is natural to test how well this works out-of-sample by evaluating

²²Recall that the explanatory variable in the estimation, $\text{RA}_{t,\tau}$, changes with the quantile level τ . Hence, based on the estimated coefficients, $\hat{\beta}_0(\tau), \hat{\beta}_1(\tau)$, we cannot tell whether the estimated quantile is monotone in τ .

Table 4: **Risk-adjusted quantile regression**

	Horizon	$\hat{\beta}_0(\tau)$	$\hat{\beta}_1(\tau)$	Wald test	$R^1(\tau)[\%]$	$R_{oos}^1(\tau)[\%]$	Obs
$\tau = 0.05$	30 days	0.29 (0.267)	0.70 (0.283)	0.09	6.28	9.94	4333
	60 days	0.30 (0.423)	0.71 (0.472)	0.08	3.4	17.81	4312
	90 days	0.36 (0.588)	0.64 (0.680)	0.08	4.26	21.98	4291
$\tau = 0.1$	30 days	0.28 (0.300)	0.72 (0.311)	0.32	3.57	4.02	4333
	60 days	0.38 (0.457)	0.61 (0.486)	0.23	2.35	9.22	4312
	90 days	0.31 (0.623)	0.70 (0.676)	0.13	4.19	13.22	4291
$\tau = 0.2$	30 days	0.57 (0.490)	0.43 (0.498)	0.47	0.58	2.53	4333
	60 days	0.44 (0.618)	0.56 (0.631)	0.37	0.57	4.28	4312
	90 days	0.23 (0.767)	0.78 (0.780)	0.58	0.7	5.99	4291

Note: This table reports the QR estimates of (4.22) over the sample period 2003-2021. Standard errors are shown in parentheses and calculated using the SETBB, with block length equal to 5 times the maturity and 1,000 Monte Carlo bootstrap samples. Wald test gives the p-value of the Wald test on the joint restriction: $\hat{\beta}_0(\tau) = 0, \hat{\beta}_1(\tau) = 1$. $R^1(\tau)$ denotes the in-sample goodness-of fit criterion (4.3). $R_{oos}^1(\tau)$ is the out-of-sample goodness-of fit (4.24), using a rolling window size of $10 \times$ maturity.

the predictive model

$$Q_{t,\tau}(R_{m,t \rightarrow N}) = \hat{Q}_{t,\tau}.$$

It is worth emphasizing that the left hand side is unknown at time t , whereas the right hand side is known at time t and does not require parameter estimation. In order to interpret $\hat{Q}_{t,\tau}$ as a valid approximation to the latent quantile function, we need to ensure that $\hat{Q}_{t,\tau}$ is not subject to the quantile crossing problem. I verify that crossing does not occur for any prediction horizon and quantile level. To asses the out-of-sample performance further, I use the following analogue of (4.4)

$$R_{oos}^1(\tau) = 1 - \frac{\sum \rho_\tau(R_{m,t \rightarrow N} - \hat{Q}_{t,\tau})}{\sum \rho_\tau(R_{m,t \rightarrow N} - \bar{Q}_{t,\tau})}. \quad (4.24)$$

The out-of-sample $R_{oos}^1(\tau)$ is also displayed in Table 4. The predictor variable $\hat{Q}_{t,\tau}$ improves upon the historical rolling quantile out-of-sample in all cases. In particular, this outperformance is most pronounced at the 5th percentile, which is expected since option data are known to provide useful information about extreme downfalls in the stock market (Bates, 2008; Bollerslev and Todorov, 2011). In Appendix E.2, I run a battery of robustness tests which show that, out-of-sample, $RA_{t,\tau}$ better predicts the quantile than other benchmarks such as the risk-neutral quantile or the VIX index.

The latter result is particularly encouraging, since the VIX predictor uses in-sample information.

4.5 Time varying disaster risk and dark matter

The in- and out-of-sample results show that $\hat{Q}_{t,\tau}$ is a good proxy for the latent conditional quantile function. Time fluctuation in $\hat{Q}_{t,\tau}$ for small τ can therefore be interpreted as time varying disaster risk. The left panels of Figure 4 show the evolution of $\hat{Q}_{t,\tau}$ over time for the 30 and 60 day horizon, with $\tau = 0.05$. The time fluctuation in both series is evident from the graph and provides empirical support for the thesis that disaster risk is time-varying, as in the models of [Gabaix \(2012\)](#) and [Wachter \(2013\)](#).

[Ross \(2015\)](#) refers to the impact that changes in perceived disaster probabilities can have on asset prices as *dark matter*: “It is unseen and not directly observable but it exerts a force that can change over time and that can profoundly influence markets”. We can illuminate this dark matter somewhat by studying the lowest quantile forecasts in Figure 4, which are produced over the 4th quarter of 2008 and the Covid crisis. During these periods, the quantile forecasts drop below 72%, which suggests that a loss of -28% or more had an expected probability of 5%. To put things in perspective, it happened only once since 1926 that the S&P500 index recorded a monthly loss of -28% or more.²³ Hence, based on historical estimates, a back of the envelope calculation puts the probability of a loss of -28% or more at 1/1139, which is 57 times lower than 5%.

The right panels of Figure 4 give another view on this dark matter, as they show the evolution of risk-adjustment over time. The largest spikes occur once more at the height of the financial crisis and the difference between the two can be as large as 25% (30 day horizon) or 16% (60 day horizon). This difference suggests that the risk-neutral quantile decreases disproportionately more than the physical quantile during crises.

It is well known that risk-neutral quantiles are smaller than historical quantiles in the left tail of the distribution. However, this fact alone does not tell us about the market’s forecast of a decline, since historical probabilities can be different from the market forecast or the risk-neutral distribution differs significantly from the physical distribution, due to a risk premium on disaster insurance. The discussion above shows that both effects are at play, but the right panels of Figure 4 suggest that the

²³I use historical monthly SP500 return from WRDS that are available from January 1926 and renders a total of 1139 observations.

insurance effect is more dominant during a crisis, since the physical and risk-neutral quantile are further apart.

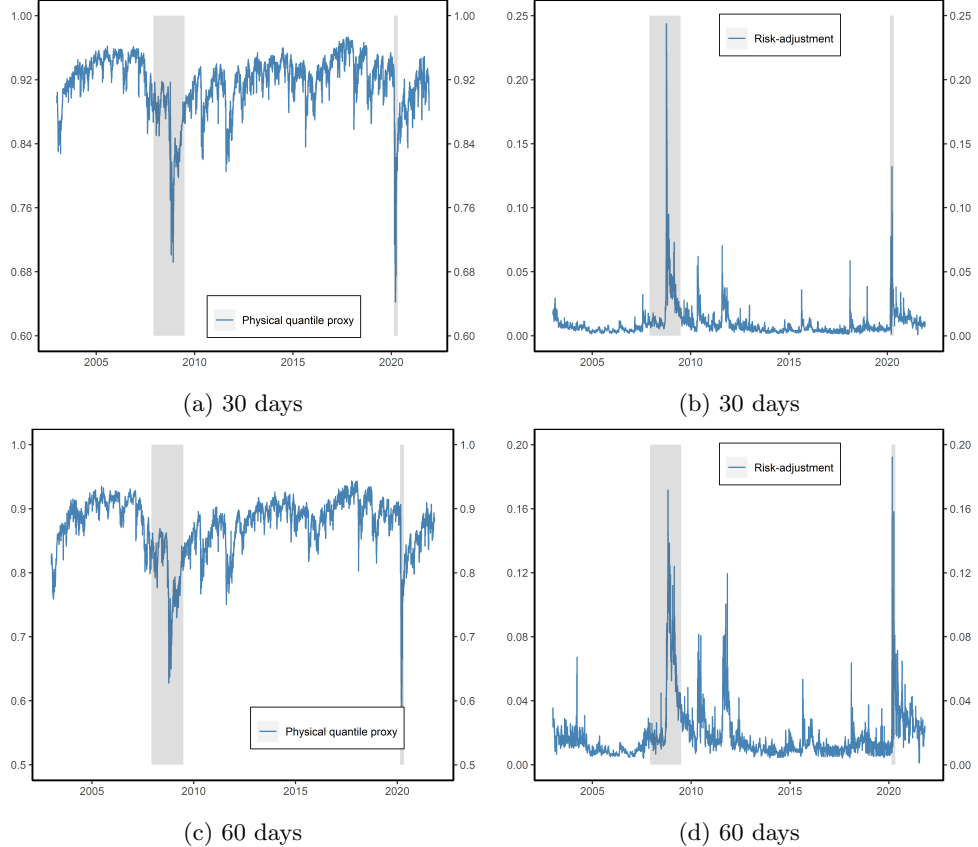


Figure 4: **Time variation in the 5th percentile at different horizons.** The left panels show the real time quantile predictor $\hat{Q}_{t,\tau}$ from (4.21) for $\tau = 0.05$. The right panels show the risk-adjustment term $RA_{t,\tau}$ from (4.17). The two shaded bars signify the Great Recession period (Dec 2007 – June 2009) and COVID-19 crisis (Feb 2020 – April 2020).

4.6 Lognormal returns and risk-neutral quantiles

Section 4.4 proposed $\hat{Q}_{t,\tau}$ as a proxy of the physical quantile function. The combined results in Tables 2 and 4 show that a risk-adjustment term is necessary in the left tail, since the risk-neutral quantile underestimates the physical quantile. In this Section, I show that the risk-neutral quantile is an optimal regressor if the data are conditionally lognormal. I verify that the risk-neutral quantile is not an optimal regressor in the data, which provides more evidence against the conditional lognormal assumption.

To describe the environment, consider the following discretized version of the Black-Scholes model. There is a riskless asset that offers a certain return, $R_f = e^{r_f \lambda}$,

and a risky asset with return $R_{m,t \rightarrow N} = \exp([\mu - \frac{1}{2}\sigma_t^2]\lambda + \sigma_t\sqrt{\lambda}Z_{t+N})$, where Z_{t+N} is standard normal, σ_t is the conditional (\mathcal{F}_t -measurable) volatility of returns and λ denotes the time difference in years between period t and $t + N$. In this setup, $M_{t \rightarrow N} := \exp(-[r_f + \xi_t^2/2]\lambda - \xi_t\sqrt{\lambda}Z_{t+N})$ is a valid SDF with conditional Sharpe ratio

$$\xi_t = \frac{\mu - r_f}{\sigma_t}.$$

The implied dynamics under risk-neutral measure are given by

$$R_{m,t \rightarrow N} = \exp\left((r_f - \frac{1}{2}\sigma_t^2)\lambda + \sigma_t\sqrt{\lambda}Z_{t+N}\right). \quad (4.25)$$

The next Proposition shows that quantile regression of the risk-neutral quantile on the return renders an identical forecast when using the (unobserved) physical quantile as a regressor.

Proposition 4.6. *Consider the lognormal model described above with return observations $\{R_{m,t \rightarrow N}\}_{t=1}^T$ stacked in the $T \times 1$ vector R . Let $\tilde{X}_t(\tau) := [1 \ \tilde{Q}_{t,\tau}(R_{m,t \rightarrow N})]$ and denote the $T \times 2$ matrix of stacked $\tilde{X}_t(\tau)$ by $\tilde{X}(\tau)$. Define the regression quantile $\hat{\beta}(\tau; R, \tilde{X}(\tau))$ as the solution to the quantile regression with the risk-neutral quantile as regressor:*

$$\hat{\beta}(\tau; R, \tilde{X}(\tau)) = \arg \min_{\beta \in \mathbb{R}^2} \sum_{t=1}^T \rho_\tau(R_{m,t \rightarrow N} - \tilde{X}_t(\tau)^\top \beta).$$

Similarly, let $X_t(\tau) := [1 \ Q_{t,\tau}(R_{m,t \rightarrow N})]$, $X(\tau)$ is the $T \times 2$ matrix of stacked $X_t(\tau)$ and define $\hat{\beta}(\tau; R, X(\tau))$ as the solution to the quantile regression using the physical quantile as regressor:

$$\hat{\beta}(\tau; R, X(\tau)) = \arg \min_{\beta \in \mathbb{R}^2} \sum_{t=1}^T \rho_\tau(R_{m,t \rightarrow N} - X_t(\tau)^\top \beta). \quad (4.26)$$

Then,

$$\tilde{X}_{T+1}(\tau)\hat{\beta}(\tau; R, \tilde{X}(\tau)) = X_{T+1}(\tau)\hat{\beta}(\tau; R, X(\tau)). \quad (4.27)$$

Proof. See Appendix A.9. ■

In sum, if returns are conditionally lognormal with time varying volatility there is no need to risk adjust, since the quantile forecast based on the risk-neutral quantile satisfies

$$Q_{T+1,\tau}(R_{m,T+1 \rightarrow N}) = \tilde{Q}_{T+1,\tau}\hat{\beta}_1(\tau) + o_p(1).$$

Intuitively, the reason is that $\hat{\beta}_1(\tau)$ picks up the risk premium, so that $\tilde{Q}_{t,\tau}\hat{\beta}_1(\tau)$ rotates back into physical quantile units. A similar situation occurs in Principal

Component Analysis, where it is enough to identify the principal component up to some rotation matrix to make predictions (Bai, 2003).

Proposition 4.6 hinges on the assumption that changes in conditional volatility is the only source of time variation in the distribution of returns. In essence, the same idea underlies the popular GARCH models. However, I have abstracted away from specifying what actually drives the volatility process, as opposed to GARCH type models.

Proposition 4.6 can be used as model free evidence against the conditional lognormal assumption. To see this, we can use QR based on the first t_0 observations to estimate the model

$$Q_{t,\tau}(R_{m,t \rightarrow N}) = \hat{\beta}_{0,t_0}(\tau) + \hat{\beta}_{1,t_0}(\tau)\tilde{Q}_{t,\tau}, \quad (4.28)$$

where the t_0 -subscript in β_{\cdot,t_0} refers to the fact that the coefficients are estimated using observations up to time t_0 . I use an expanding window to estimate β_{\cdot,t_0} in (4.28), which are used to produce dynamic quantile forecasts of the form

$$\hat{Q}_{t,\tau}^{\text{logn}} = \hat{\beta}_{0,t}(\tau) + \hat{\beta}_{1,t}(\tau)\tilde{Q}_{t,\tau}. \quad (4.29)$$

If returns follow the lognormal dynamics in (4.25), Proposition 4.6 suggests that

$$Q_{t,\tau}(R_{m,t \rightarrow N}) \approx \hat{Q}_{t,\tau}^{\text{logn}}.$$

This approximation can be formalized by testing the joint restriction

$$H_0 : [\beta_0(\tau), \beta_1(\tau)] = [0, 1]^\top, \quad (4.30)$$

in the quantile regression

$$\min_{\beta_0, \beta_1 \in \mathbb{R}} \sum_t \rho_\tau \left(R_{m,t \rightarrow N} - \beta_0 - \beta_1 \hat{Q}_{t,\tau}^{\text{logn}} \right).$$

The results are summarized in Table 5. The point estimates are quite far from the $[0, 1]^\top$ benchmark, especially compared to Table 4. The Wald test on the joint restriction is rejected for $\tau \in \{0.05, 0.1\}$, but fails to reject for $\tau = 0.2$ at both prediction horizons. Additionally, the explanatory power is low relative to Table 4, as can be seen from the $R^1(\tau)$ statistic. These numbers provide strong evidence against the conditional lognormal assumption, which is in line with our results from Section 4.2 and evidence from the literature (see e.g. Martin (2017, Result 4)).

Table 5: Expanding quantile prediction with risk-neutral quantile

	Horizon	$\hat{\beta}_0(\tau)$	$\hat{\beta}_1(\tau)$	Wald test	$R^1(\tau)[\%]$	Obs
$\tau = 0.05$	30 days	0.54 (0.186)	0.42 (0.194)	0	4.36	3804
	60 days	0.55 (0.293)	0.39 (0.314)	0.11	1.84	3753
	90 days	0.78 (0.335)	0.11 (0.353)	0.01	0.88	3702
$\tau = 0.1$	30 days	0.59 (0.233)	0.39 (0.240)	0.03	2.39	3804
	60 days	0.80 (0.382)	0.16 (0.397)	0.06	0.22	3753
	90 days	0.74 (0.416)	0.21 (0.433)	0.09	1.34	3702
$\tau = 0.2$	30 days	0.83 (0.422)	0.15 (0.429)	0.14	0.28	3804
	60 days	0.87 (0.508)	0.11 (0.517)	0.23	0.25	3753
	90 days	0.73 (0.528)	0.26 (0.534)	0.37	0.52	3702

Note: This table reports the QR estimates of (4.29) using an expanding window based on an initial 500 observations. The sample period is 2003-2021. Wald test denotes the p -value of the joint restriction $[\beta_0(\tau), \beta_1(\tau)]^\top = [0, 1]^\top$. Standard errors are reported in parentheses and calculated using the SETBB with a block length of 5 times the prediction horizon. $R^1(\tau)$ denotes the goodness of fit measure (4.3).

5 Conclusion

This paper proposes a new bound (quantile bound) on the SDF volatility which, unlike the HJ bound, compares the physical and risk-neutral distribution at every τ -quantile. I interpret the quantile bound as a local version of the HJ bound and show that the quantile bound compares favorably to the HJ bound in models that incorporate disaster risk. This result is driven by relatively large differences between the physical and risk-neutral distribution in the left tail. I also advocate to use the shape of the quantile bound to diagnose misspecification of asset pricing models.

In the data, I find suggestive evidence of the presence of disaster risk and show that the quantile bound is stronger than the HJ bound. This empirical finding puts a tight constraint on the risk-aversion coefficient of a representative agent in asset pricing models that do not incorporate disaster risk. Specifically, in the LRR model, the quantile bound cannot overcome the HJ bound for any reasonable level of risk-aversion.

Subsequently, I analyze the conditional difference between the physical and risk-neutral quantile. A quantile regression of the risk-neutral quantile on the returns pro-

vides new empirical evidence, which shows that most risk-adjustment is coming from the left tail of the return distribution. I propose a nonparametric risk-adjustment term that captures most of the difference between the physical and risk-neutral distribution in the left tail. This difference fluctuates significantly over time and spikes during crises, which is model-free evidence of time varying disaster risk. Moreover, these spikes suggest that during a crisis, the left tails of physical and risk-neutral distribution differ more.

I propose several in- and out-of-sample metrics that demonstrate the power of my nonparametric approach over competing benchmarks. These metrics generalize some of the common evaluation techniques in the return prediction literature to the quantile setting. I find, using these new measures, that the risk-adjustment term predicts the difference between physical and risk-neutral quantile well. Overall, the results underscore the importance of considering features of the data beyond the mean and variance and provide deeper insight in the influence of tail risk on asset prices.

References

Yacine Aït-Sahalia and Andrew W. Lo. Nonparametric estimation of state-price densities implicit in financial asset prices. *Journal of Finance*, 53(2):499–547, 1998. doi:[10.1111/0022-1082.215228](https://doi.org/10.1111/0022-1082.215228).

Yacine Aït-Sahalia and Andrew W. Lo. Nonparametric risk management and implied risk aversion. *Journal of Econometrics*, 94(1):9–51, 2000. doi:[10.1016/S0304-4076\(99\)00016-0](https://doi.org/10.1016/S0304-4076(99)00016-0).

Caio Almeida and René Garcia. Assessing misspecified asset pricing models with empirical likelihood estimators. *Journal of Econometrics*, 170(2):519–537, 2012. doi:[10.1016/j.jeconom.2012.05.020](https://doi.org/10.1016/j.jeconom.2012.05.020).

Fernando Alvarez and Urban J. Jermann. Using asset prices to measure the persistence of the marginal utility of wealth. *Econometrica*, 73(6):1977–2016, 2005. doi:[10.1111/j.1468-0262.2005.00643.x](https://doi.org/10.1111/j.1468-0262.2005.00643.x).

Joshua Angrist, Victor Chernozhukov, and Iván Fernández-Val. Quantile regression under misspecification, with an application to the U.S. wage structure. *Econometrica*, 74(2):539–563, 2006. doi:[10.1111/j.1468-0262.2006.00671.x](https://doi.org/10.1111/j.1468-0262.2006.00671.x).

David Backus, Mikhail Chernov, and Ian Martin. Disasters implied by equity index options. *Journal of Finance*, 66(6):1969–2012, 2011. doi:[10.1111/j.1540-6261.2011.01697.x](https://doi.org/10.1111/j.1540-6261.2011.01697.x).

David Backus, Mikhail Chernov, and Stanley Zin. Sources of entropy in representative agent models. *Journal of Finance*, 69(1):51–99, 2014. doi:[10.1111/jofi.12090](https://doi.org/10.1111/jofi.12090).

Jushan Bai. Inferential theory for factor models of large dimensions. *Econometrica*, 71(1):135–171, 2003. doi:[10.1111/1468-0262.00392](https://doi.org/10.1111/1468-0262.00392).

Gurdip Bakshi and Fousseni Chabi-Yo. Variance bounds on the permanent and transitory components of stochastic discount factors. *Journal of Financial Economics*, 105(1):191–208, 2012. doi:[10.1016/j.jfineco.2012.01.003](https://doi.org/10.1016/j.jfineco.2012.01.003).

Gurdip Bakshi, Dilip Madan, and George Panayotov. Returns of claims on the upside and the viability of U-shaped pricing kernels. *Journal of Financial Economics*, 97(1):130–154, 2010. doi:[10.1016/j.jfineco.2010.03.009](https://doi.org/10.1016/j.jfineco.2010.03.009).

Ravi Bansal and Bruce N. Lehmann. Growth-optimal portfolio restrictions on asset pricing models. *Macroeconomic Dynamics*, 1(2):333–354, 1997. doi:[10.1017/S1365100597003039](https://doi.org/10.1017/S1365100597003039).

Ravi Bansal and Amir Yaron. Risks for the long run: A potential resolution of asset pricing puzzles. *Journal of Finance*, 59(4):1481–1509, 2004. doi:[10.1111/j.1540-6261.2004.00670.x](https://doi.org/10.1111/j.1540-6261.2004.00670.x).

Ravi Bansal, Dana Kiku, and Amir Yaron. An empirical evaluation of the long-run risks model for asset prices. *Critical Finance Review*, 1(1):183–221, 2012. doi:[10.1561/103.00000005](https://doi.org/10.1561/103.00000005).

Andrea Barletta and Paolo Santucci de Magistris. Analyzing the risks embedded in option prices with *rndfittool*. *Risks*, 6(2):1–15, 2018. doi:[10.3390/risks6020028](https://doi.org/10.3390/risks6020028).

Robert J. Barro. Rare disasters and asset markets in the twentieth century. *Quarterly Journal of Economics*, 121(3):823–866, 2006. doi:[10.1162/qjec.121.3.823](https://doi.org/10.1162/qjec.121.3.823).

David S. Bates. The crash of '87: was it expected? The evidence from options markets. *Journal of Finance*, 46(3):1009–1044, 1991. doi:[10.1111/j.1540-6261.1991.tb03775.x](https://doi.org/10.1111/j.1540-6261.1991.tb03775.x).

David S. Bates. Post-'87 crash fears in the S&P500 futures option market. *Journal of Econometrics*, 94(1):181–238, 2000. doi:[10.1016/S0304-4076\(99\)00021-4](https://doi.org/10.1016/S0304-4076(99)00021-4).

David S. Bates. The market for crash risk. *Journal of Economic Dynamics and Control*, 32(7):2291–2321, 2008. doi:[10.1016/j.jedc.2007.09.020](https://doi.org/10.1016/j.jedc.2007.09.020).

Brendan K. Beare and Lawrence D. W. Schmidt. An empirical test of pricing kernel monotonicity. *Journal of Applied Econometrics*, 31(2):338–356, 2016. doi:[10.1002/jae.2422](https://doi.org/10.1002/jae.2422).

Geert Bekaert and Marie Hoerova. The VIX, the variance premium and stock market volatility. *Journal of Econometrics*, 183(2):181–192, 2014. doi:[10.1016/j.jeconom.2014.05.008](https://doi.org/10.1016/j.jeconom.2014.05.008).

Fischer Black and Myron Scholes. The pricing of options and corporate liabilities. *Journal of Political Economy*, 81(3):637–654, 1973. doi:[10.1086/260062](https://doi.org/10.1086/260062).

Tim Bollerslev and Viktor Todorov. Tails, fears, and risk premia. *Journal of Finance*, 66(6):2165–2211, 2011. doi:[10.1111/j.1540-6261.2011.01695.x](https://doi.org/10.1111/j.1540-6261.2011.01695.x).

Jaroslav Borovička, Lars Peter Hansen, and José A Scheinkman. Misspecified recovery. *Journal of Finance*, 71(6):2493–2544, 2016. doi:[10.1111/jofi.12404](https://doi.org/10.1111/jofi.12404).

Douglas T. Breeden and Robert H. Litzenberger. Prices of state-contingent claims implicit in option prices. *Journal of Business*, 51(4):621–651, 1978. doi:[10.1086/296025](https://doi.org/10.1086/296025).

Mark Broadie, Mikhail Chernov, and Michael Johannes. Understanding index option returns. *Review of Financial Studies*, 22(11):4493–4529, 2009. doi:[10.1093/rfs/hhp032](https://doi.org/10.1093/rfs/hhp032).

John Y. Campbell and Samuel B. Thompson. Predicting excess stock returns out of sample: Can anything beat the historical average? *Review of Financial Studies*, 21(4):1509–1531, 2008. doi:[10.1093/rfs/hhm055](https://doi.org/10.1093/rfs/hhm055).

George Casella and Roger L. Berger. *Statistical Inference*. Duxbury/Thomson Learning, Belmont, CA, 2002.

Fousseni Chabi-Yo and Johnathan Loudis. The conditional expected market return. *Journal of Financial Economics*, 137(3):752–786, 2020. doi:[10.1016/j.jfineco.2020.03.009](https://doi.org/10.1016/j.jfineco.2020.03.009).

Liang Chen, Juan J. Dolado, and Jesús Gonzalo. Quantile factor models. *Econometrica*, 89(2):875–910, 2021. doi:[10.3982/ECTA15746](https://doi.org/10.3982/ECTA15746).

Victor Chernozhukov, Iván Fernández-Val, and Siyi Luo. Distribution regression with sample selection, with an application to wage decompositions in the UK, 2018. URL <https://arxiv.org/abs/1811.11603>.

John H. Cochrane. *Asset Pricing*. Princeton University Press, 2005.

Joshua D. Coval and Tyler Shumway. Expected option returns. *Journal of Finance*, 56(3):983–1009, 2001. doi:[10.1111/0022-1082.00352](https://doi.org/10.1111/0022-1082.00352).

Horatio Cuesdeanu and Jens Carsten Jackwerth. The pricing kernel puzzle in forward looking data. *Review of Derivatives Research*, 21(3):253–276, 2018. doi:[10.1007/s11147-017-9140-8](https://doi.org/10.1007/s11147-017-9140-8).

Jon Danielsson and Casper G. de Vries. Value-at-risk and extreme returns. *Annales d'Économie et de Statistique*, (60):239–270, 2000. doi:[10.2307/20076262](https://doi.org/10.2307/20076262).

Larry G. Epstein and Stanley E. Zin. Substitution, risk aversion and the temporal behavior of consumption and asset returns: A theoretical framework. *Econometrica*, 57(4):937–969, 1989. doi:[10.2307/1913778](https://doi.org/10.2307/1913778).

Stephen Figlewski. Estimating the implied risk-neutral density for the US market portfolio. In *Volatility and Time Series Econometrics: Essays in Honor of Robert Engle*, chapter 15, pages 323–353. Oxford University Press, 03 2010. doi:[10.1093/acprof:oso/9780199549498.003.0015](https://doi.org/10.1093/acprof:oso/9780199549498.003.0015).

Damir Filipović, Eberhard Mayerhofer, and Paul Schneider. Density approximations for multivariate affine jump-diffusion processes. *Journal of Econometrics*, 176(2):93–111, 2013. doi:[10.1016/j.jeconom.2012.12.003](https://doi.org/10.1016/j.jeconom.2012.12.003).

Xavier Gabaix. Variable rare disasters: An exactly solved framework for ten puzzles in macro-finance. *Quarterly Journal of Economics*, 127(2):645–700, 2012. doi:[10.1093/qje/qjs001](https://doi.org/10.1093/qje/qjs001).

Can Gao and Ian Martin. Volatility, valuation ratios, and bubbles: An empirical measure of market sentiment. *Journal of Finance*, 76(6):3211–3254, 2021. doi:[10.1111/jofi.13068](https://doi.org/10.1111/jofi.13068).

Christian Gouriéroux and Joann Jasiak. Dynamic quantile models. *Journal of Econometrics*, 147(1):198–205, 2008. doi:[10.1016/j.jeconom.2008.09.028](https://doi.org/10.1016/j.jeconom.2008.09.028).

Karl B. Gregory, Soumendra N. Lahiri, and Daniel J. Nordman. A smooth block bootstrap for quantile regression with time series. *Annals of Statistics*, 46(3):1138–1166, 2018. doi:[10.1214/17-AOS1580](https://doi.org/10.1214/17-AOS1580).

Lars Peter Hansen and Robert J. Hodrick. Forward exchange rates as optimal predictors of future spot rates: An econometric analysis. *Journal of Political Economy*, 88(5):829–853, 1980. doi:[10.1086/260910](https://doi.org/10.1086/260910).

Lars Peter Hansen and Ravi Jagannathan. Implications of security market data for models of dynamic economies. *Journal of Political Economy*, 99(2):225–262, 1991. doi:[10.1086/261749](https://doi.org/10.1086/261749).

Fushing Hsieh and Bruce W. Turnbull. Nonparametric and semiparametric estimation of the receiver operating characteristic curve. *Annals of Statistics*, 24(1):25–40, 1996. doi:[10.1214/aos/1033066197](https://doi.org/10.1214/aos/1033066197).

Elton P. Hsu and S. R. Srinivasa Varadhan. *Probability Theory and Applications*. American Mathematical Society, 1999.

Jens Carsten Jackwerth. Recovering risk aversion from option prices and realized returns. *Review of Financial Studies*, 13(2):433–451, 2000. doi:[10.1093/rfs/13.2.433](https://doi.org/10.1093/rfs/13.2.433).

Jens Carsten Jackwerth and Marco Menner. Does the Ross recovery theorem work empirically? *Journal of Financial Economics*, 137(3):723–739, 2020. doi:[10.1016/j.jfineco.2020.03.006](https://doi.org/10.1016/j.jfineco.2020.03.006).

Roger Koenker and Gilbert Bassett. Regression quantiles. *Econometrica*, 46(1):33–50, 1978. doi:[10.2307/1913643](https://doi.org/10.2307/1913643).

Roger Koenker and José A. F. Machado. Goodness of fit and related inference processes for quantile regression. *Journal of the American Statistical Association*, 94(448):1296–1310, 1999. doi:[10.1080/01621459.1999.10473882](https://doi.org/10.1080/01621459.1999.10473882).

Erich L. Lehmann. Some concepts of dependence. *Annals of Mathematical Statistics*, 37(5):1137–1153, 1966. doi:[10.1214/aoms/1177699260](https://doi.org/10.1214/aoms/1177699260).

Matthew Linn, Sophie Shive, and Tyler Shumway. Pricing kernel monotonicity and conditional information. *Review of Financial Studies*, 31(2):493–531, 2018. doi:[10.1093/rfs/hhx095](https://doi.org/10.1093/rfs/hhx095).

Yan Liu. Index option returns and generalized entropy bounds. *Journal of Financial Economics*, 139(3):1015–1036, 2021. doi:[10.1016/j.jfineco.2020.08.011](https://doi.org/10.1016/j.jfineco.2020.08.011).

Ian Martin. Consumption-based asset pricing with higher cumulants. *Review of Economic Studies*, 80(2):745–773, 2013. doi:[10.1093/restud/rds029](https://doi.org/10.1093/restud/rds029).

Ian Martin. What is the expected return on the market? *Quarterly Journal of Economics*, 132(1):367–433, 2017. doi:[10.1093/qje/qjw034](https://doi.org/10.1093/qje/qjw034).

Ian Martin and Christian Wagner. What is the expected return on a stock? *Journal of Finance*, 74(4):1887–1929, 2019. doi:[10.1111/jofi.12778](https://doi.org/10.1111/jofi.12778).

William A. Massey and Ward Whitt. A probabilistic generalization of Taylor’s theorem. *Statistics & Probability Letters*, 16(1):51–54, 1993. doi:[10.1016/0167-7152\(93\)90122-Y](https://doi.org/10.1016/0167-7152(93)90122-Y).

Alexander J. McNeil, Rüdiger Frey, and Paul Embrechts. *Quantitative Risk Management: Concepts, Techniques and Tools*. Princeton University Press, 2015.

Dimitris N. Politis and Joseph P. Romano. The stationary bootstrap. *Journal of the American Statistical Association*, 89(428):1303–1313, 1994. doi:[10.1080/01621459.1994.10476870](https://doi.org/10.1080/01621459.1994.10476870).

Likuan Qin and Vadim Linetsky. Long-term risk: A martingale approach. *Econometrica*, 85(1):299–312, 2017. doi:[10.3982/ECTA13438](https://doi.org/10.3982/ECTA13438).

Likuan Qin, Vadim Linetsky, and Yutian Nie. Long forward probabilities, recovery, and the term structure of bond risk premiums. *Review of Financial Studies*, 31(12):4863–4883, 2018. doi:[10.1093/rfs/hhy042](https://doi.org/10.1093/rfs/hhy042).

Thomas A. Rietz. The equity risk premium a solution. *Journal of Monetary Economics*, 22(1):117–131, 1988. doi:[10.1016/0304-3932\(88\)90172-9](https://doi.org/10.1016/0304-3932(88)90172-9).

Joshua V. Rosenberg and Robert F. Engle. Empirical pricing kernels. *Journal of Financial Economics*, 64(3):341–372, 2002. doi:[10.1016/S0304-405X\(02\)00128-9](https://doi.org/10.1016/S0304-405X(02)00128-9).

Stephen A. Ross. *Neoclassical Finance*. Princeton University Press, 2005.

Stephen A. Ross. The recovery theorem. *Journal of Finance*, 70(2):615–648, 2015. doi:[10.1111/jofi.12092](https://doi.org/10.1111/jofi.12092).

Robert J. Serfling. *Approximation Theorems of Mathematical Statistics*. John Wiley & Sons, 2009.

Karl N. Snow. Diagnosing asset pricing models using the distribution of asset returns. *Journal of Finance*, 46(3):955–983, 1991. doi:[10.1111/j.1540-6261.1991.tb03773.x](https://doi.org/10.1111/j.1540-6261.1991.tb03773.x).

Michael Stutzer. A Bayesian approach to diagnosis of asset pricing models. *Journal of Econometrics*, 68(2):367–397, 1995. doi:[10.1016/0304-4076\(94\)01656-K](https://doi.org/10.1016/0304-4076(94)01656-K).

Engin A. Sungur. Dependence information in parameterized copulas. *Communications in Statistics - Simulation and Computation*, 19(4):1339–1360, 1990. doi:[10.1080/03610919008812920](https://doi.org/10.1080/03610919008812920).

Aad W. van der Vaart. *Asymptotic Statistics*. Cambridge University Press, 2000.

Jessica A. Wachter. Can time-varying risk of rare disasters explain aggregate stock market volatility? *Journal of Finance*, 68(3):987–1035, 2013. doi:[10.1111/jofi.12018](https://doi.org/10.1111/jofi.12018).

Ivo Welch and Amit Goyal. A comprehensive look at the empirical performance of equity premium prediction. *Review of Financial Studies*, 21(4):1455–1508, 2008. doi:[10.1093/rfs/hhm014](https://doi.org/10.1093/rfs/hhm014).

A Proofs

This Section contains proofs and detailed calculations of results used in the main paper.

A.1 Proof of Theorem 2.1

Proof. I suppress the dependence of the τ -quantile on R and write $\tilde{Q}_\tau := \tilde{Q}_\tau(R)$. Starting from the definition of a risk-neutral quantile, I obtain

$$\begin{aligned}\tau &= \tilde{\mathbb{P}}[R \leq \tilde{Q}_\tau] = \tilde{\mathbb{E}}[\mathbb{1}(R \leq \tilde{Q}_\tau)] = R_f \mathbb{E}[M \mathbb{1}(R \leq \tilde{Q}_\tau)] \\ &= R_f [\mathbb{COV}(M, \mathbb{1}(R \leq \tilde{Q}_\tau)) + \mathbb{E}[M] \mathbb{E}[\mathbb{1}(R \leq \tilde{Q}_\tau)]] \\ &= R_f \mathbb{COV}(M, \mathbb{1}(R \leq \tilde{Q}_\tau)) + \underbrace{\mathbb{E}[\mathbb{1}(R \leq \tilde{Q}_\tau)]}_{=\phi(\tau)}.\end{aligned}\tag{A.1}$$

Rearranging then yields

$$\frac{\tau - \phi(\tau)}{R_f} = \mathbb{COV}(M, \mathbb{1}(R \leq \tilde{Q}_\tau)).$$

Using Cauchy-Schwarz renders the inequality

$$\begin{aligned}\frac{|\tau - \phi(\tau)|}{R_f} &\leq \sigma(M) \sigma(\mathbb{1}(R \leq \tilde{Q}_\tau)) \\ \frac{|\tau - \phi(\tau)|}{\sigma(\mathbb{1}(R \leq \tilde{Q}_\tau)) R_f} &\leq \sigma(M).\end{aligned}\tag{A.2}$$

Finally, since $\mathbb{1}(R \leq \tilde{Q}_\tau)$ is a Bernoulli random variable, it follows that

$$\sigma(\mathbb{1}(R \leq \tilde{Q}_\tau)) = \sqrt{\phi(\tau)(1 - \phi(\tau))}.\tag{A.3}$$

Theorem 2.1 now follows after substituting (A.3) into (A.2). ■

A.2 Quantile bound Pareto distribution

Proof of Proposition 2.3. (i) The distribution of returns is Pareto, since

$$\begin{aligned}\mathbb{P}(R \leq x) &= \mathbb{P}(U^{-\beta} \leq x/B) \\ &= \mathbb{P}\left(U \geq (x/B)^{-\frac{1}{\beta}}\right) = 1 - \left(\frac{x}{B}\right)^{-\frac{1}{\beta}}, \quad x \geq B.\end{aligned}$$

(ii) Since $R_f M$ is the Radon-Nikodym derivative that induces a change of measure

from \mathbb{P} to $\tilde{\mathbb{P}}$, it follows that

$$\begin{aligned}
\tilde{\mathbb{P}}(R \leq x) &= R_f \mathbb{E}[M \mathbb{1}(R \leq x)] \\
&= R_f \int_0^1 A u^\alpha \mathbb{1}(B u^{-\beta} \leq x) du \\
&= R_f A \int_0^1 u^\alpha \mathbb{1}\left(u \geq \left(\frac{x}{B}\right)^{-\frac{1}{\beta}}\right) du \\
&= \frac{R_f A}{\alpha + 1} \left(1 - \left(\frac{x}{B}\right)^{-\frac{\alpha+1}{\beta}}\right) \\
&= 1 - \left(\frac{x}{B}\right)^{-\frac{\alpha+1}{\beta}}.
\end{aligned}$$

The last line follows from (A.6).

(iii) Routine calculations show that the mean and variance of R are given by (provided $\beta < 1/2$)

$$\mathbb{E}[R] = \frac{B}{1-\beta} \quad \sigma^2(R) = \frac{B^2}{1-2\beta} - \left(\frac{B}{1-\beta}\right)^2. \quad (\text{A.4})$$

Likewise, the distribution of the SDF follows from

$$\mathbb{P}(M \leq x) = \mathbb{P}(AU^\alpha \leq x) = \left(\frac{x}{A}\right)^{\frac{1}{\alpha}}, \quad 0 \leq x \leq A.$$

In this case, M is said to have a Pareto lower tail. The expectation is given by

$$\mathbb{E}[M] = \frac{A}{\alpha + 1}.$$

The constraint $\mathbb{E}[MR] = 1$ forces

$$\frac{AB}{\alpha - \beta + 1} = 1. \quad (\text{A.5})$$

In addition from $\mathbb{E}[M] = \frac{1}{R_f}$ it follows

$$\frac{A}{\alpha + 1} = \frac{1}{R_f}. \quad (\text{A.6})$$

The Sharpe ratio can now be computed from (A.4) and (A.6).

(iv) It is straightforward to show that the quantiles of a **Par** (C, ζ) distribution are given by

$$Q_\tau = C \times (1 - \tau)^{-1/\zeta}.$$

It therefore follows that the risk-neutral quantile function is equal to

$$\tilde{Q}_\tau = B(1 - \tau)^{-\frac{\beta}{\alpha+1}}.$$

As a result

$$\begin{aligned}\mathbb{P}(R \leq \tilde{Q}_\tau) &= \mathbb{P}\left(R \leq B(1 - \tau)^{-\frac{\beta}{\alpha+1}}\right) \\ &= 1 - \left(\frac{B}{B(1 - \tau)^{\frac{-\beta}{\alpha+1}}}\right)^{\frac{1}{\beta}} \\ &= 1 - (1 - \tau)^{\frac{1}{\alpha+1}}.\end{aligned}$$

Hence, the quantile bound evaluates to

$$\frac{1}{R_f} \frac{|\tau - \phi(\tau)|}{\sqrt{\phi(\tau)(1 - \phi(\tau))}} = \frac{A}{1 + \alpha} \frac{\left|\tau - 1 + (1 - \tau)^{\frac{1}{\alpha+1}}\right|}{\sqrt{(1 - (1 - \tau)^{\frac{1}{\alpha+1}})(1 - \tau)^{\frac{1}{\alpha+1}}}}.$$

(v) The HJ bound, as given by the Sharpe ratio in (2.15), goes to 0 as $\beta \uparrow 1/2$ since $\sigma(R) \uparrow \infty$. ■

A.3 Jointly normal return and SDF

In this Section, I prove (2.11) and (2.10), when M and R are jointly normal. First I derive (2.11). The proof of the quantile bound in Theorem 2.1 gives the following identity

$$\frac{|\tau - \phi(\tau)|}{R_f} = |\mathbb{COV}\left(\mathbb{1}(R \leq \tilde{Q}_\tau), M\right)|.$$

Standard SDF properties also yield the well known result

$$\frac{|\mathbb{E}(R) - R_f|}{R_f} = |\mathbb{COV}(R, M)|.$$

These results, combined with (2.10) prove (2.11), since

$$\begin{aligned}\frac{\text{HJ bound}}{\text{Quantile bound}} &= \frac{\frac{|\mathbb{E}(R) - R_f|}{\sigma_R R_f}}{\frac{|\tau - \phi(\tau)|}{\sqrt{\phi(\tau)(1 - \phi(\tau))} R_f}} \\ &\stackrel{(2.10)}{=} \frac{\sqrt{\phi(\tau)(1 - \phi(\tau))}}{\sigma_R f_R(\tilde{Q}_\tau)},\end{aligned}$$

where $f_R(\tilde{Q}_\tau)$ is the marginal density of R .

It remains to prove (2.10). I make use of the following covariance identities, which are due to W. Hoeffding.

Lemma A.1 (Hoeffding). *For any integrable random variable X and Z with marginal CDFs F_X, F_Z and joint CDF $F_{X,Z}$, it holds that*

$$\text{COV}[\mathbb{1}(Z \leq z), X] = - \int_{-\infty}^{\infty} [F_{X,Z}(x, z) - F_X(x)F_Z(z)] dx \quad (\text{A.7})$$

$$\text{COV}[Z, X] = - \int_{-\infty}^{\infty} \text{COV}[\mathbb{1}(Z \leq z), X] dz. \quad (\text{A.8})$$

Proof. See [Lehmann \(1966\)](#). ■

I also need a relation for the bivariate normal distribution. Suppose that X, Z are jointly normal with correlation ρ , mean μ_X, μ_Z and variance σ_X^2, σ_Z^2 , then ([Sungur, 1990](#))

$$\frac{\partial \Phi_2(x, z; \rho, \mu_X, \mu_Z, \sigma_X^2, \sigma_Z^2)}{\partial \rho} = \sigma_X \sigma_Z \phi_2(x, z; \rho, \mu_X, \mu_Z, \sigma_X^2, \sigma_Z^2), \quad (\text{A.9})$$

where $\Phi_2(\cdot)$ denotes the bivariate normal CDF and $\phi_2(\cdot)$ denotes the bivariate normal PDF. We can now prove a covariance identity for jointly normal random variables.

Proposition A.2. *Suppose R and M are jointly normal with correlation ρ , then*

$$-\text{COV}[\mathbb{1}(R \leq x), M] = \phi_R(x) \cdot \text{COV}[R, M], \quad (\text{A.10})$$

where $\phi_R(\cdot)$ is the marginal density of R .

Proof. To lighten notation, I suppress the dependence on $\mu_R, \mu_M, \sigma_R^2, \sigma_M^2$ in the joint CDF and PDF. We then have

$$\begin{aligned} -\text{COV}[\mathbb{1}(R \leq x), M] &= \int_{-\infty}^{\infty} \Phi_2(x, m; \rho) - \Phi_2(x, m; 0) dm \\ &= \int_{-\infty}^{\infty} \int_0^{\rho} \sigma_R \sigma_M \phi_2(x, m; y) dy dm \\ &= \sigma_R \sigma_M \rho \phi_R(x) = \text{COV}[M, R] \phi_R(x), \end{aligned}$$

where, in the first line, I use (A.7) together with $F_R(r)F_M(m) = \Phi_2(r, m; 0)$, the second line follows from (A.9) and the third line follows from Fubini's theorem to swap the order of integration and $\int_{-\infty}^{\infty} \phi_2(x, m; y) dm = \phi_R(x)$. ■

Remark. The second covariance identity in (A.8) shows that $\text{COV}[\mathbb{1}(R \leq x), M]$ is a measure of local dependence. In case of joint normality (A.10), the weight is given by the marginal PDF. For other distributions, the weighting factor is more complicated,

but sometimes can be given an explicit form using a *local Gaussian representation* (see [Chernozhukov et al. \(2018\)](#)).

A.4 Lognormal return and SDF

This Section provides a closed form approximation for the relative efficiency between the HJ and quantile bound under joint lognormality. Recall the distribution assumption

$$R = e^{(\mu_R - \frac{\sigma_R^2}{2})\lambda + \sigma_R \sqrt{\lambda} Z_R}$$

$$M = e^{-(r_f + \frac{\sigma_M^2}{2})\lambda + \sigma_M \sqrt{\lambda} Z_M}.$$

Both Z_R and Z_M are standard normal random variables with correlation ρ . First, approximate M by a first order Taylor expansion, which gives

$$\widehat{M} = e^{-(r_f + \frac{\sigma_M^2}{2})\lambda} + Z_M \sigma_M \sqrt{\lambda} e^{-(r_f + \frac{\sigma_M^2}{2})\lambda}.$$

Notice that $\widehat{M} = M + o_p(\sqrt{\lambda})$. Consequently, by Stein's Lemma

$$\begin{aligned} \mathbb{COV}(R, M) &\approx \mathbb{COV}(R, \widehat{M}) = \sigma_M \sqrt{\lambda} e^{-(r_f + \frac{\sigma_M^2}{2})\lambda} \mathbb{COV}(R, Z_M) \\ &= \sigma_M \sqrt{\lambda} e^{-(r_f + \frac{\sigma_M^2}{2})\lambda} \mathbb{E} \left[\sigma_R \sqrt{\lambda} \exp \left(\left[\mu_R - \frac{\sigma_R^2}{2} \right] \lambda + \sigma_R \sqrt{\lambda} Z_R \right) \right] \mathbb{COV}(Z_R, Z_M) \\ &= \sigma_M \sigma_R \lambda e^{-(r_f + \frac{\sigma_M^2}{2})\lambda} e^{\mu_R \lambda} \mathbb{COV}(Z_R, Z_M). \end{aligned}$$

By Proposition [A.2](#),

$$\begin{aligned} \mathbb{COV}(\mathbb{1}(\log R \leq x), M) &\approx \mathbb{COV}(\mathbb{1}(\log R \leq x), \widehat{M}) \\ &= \sigma_M \sqrt{\lambda} e^{-(r_f + \frac{\sigma_M^2}{2})\lambda} \mathbb{COV}(\mathbb{1}(\log R \leq x), Z_M) \\ &= \sigma_M \sqrt{\lambda} e^{-(r_f + \frac{\sigma_M^2}{2})\lambda} \mathbb{COV}(\mathbb{1}((\mu_R - \sigma_R^2/2)\lambda + \sigma_R \sqrt{\lambda} Z_R \leq x), Z_M) \\ &= -\sigma_M \sqrt{\lambda} e^{-(r_f + \frac{\sigma_M^2}{2})\lambda} f(x) \mathbb{COV}(Z_R, Z_M). \end{aligned}$$

Here, f is the density of a normal random variable with mean $(\mu_R - \sigma_R^2/2)\lambda$ and variance $\lambda\sigma_R^2$. As a result,

$$\left| \frac{\mathbb{E}[R] - e^{\lambda r_f}}{\tau - \phi(\tau)} \right| \approx \frac{\sigma_R \sqrt{\lambda} e^{\mu_R \lambda}}{f(x)}. \quad (\text{A.11})$$

The same reasoning in Example 2.2 implies that the relative efficiency between the HJ and quantile bound can be approximated by

$$\frac{\text{HJ bound}}{\text{Quantile bound}} = \frac{\frac{|\mathbb{E}[R] - R_f|}{\sigma(R)R_f}}{\frac{|\tau - \phi(\tau)|}{\sqrt{\phi(\tau)(1 - \phi(\tau))R_f}}} \quad (\text{A.12})$$

$$\stackrel{(\text{A.11})}{\approx} \frac{\sqrt{\mathbb{P}(r \leq x) \cdot (1 - \mathbb{P}(r \leq x))}}{\sigma(R)} \times \frac{\sigma_R \sqrt{\lambda} e^{\mu_R \lambda}}{f(x)}, \quad (\text{A.13})$$

where $r = \log R$ and $x = \log \tilde{Q}_\tau$. Using the same reasoning as in Example 2.2, the expression on the right hand side of (A.12) is minimized by choosing $x = \log \tilde{Q}_\tau^*$ s.t. $\mathbb{P}(R \leq \tilde{Q}_\tau^*) = 1/2$. In that case the relative efficiency equals

$$\frac{\sqrt{2\pi\sigma_R^2 \sqrt{\lambda} e^{\mu_R \lambda}}}{2\sqrt{[\exp(\sigma_R^2 \lambda) - 1] \exp(2\mu_R \lambda)}} = \frac{1}{2} \sqrt{\frac{2\pi\sigma_R^2 \lambda}{\exp(\sigma_R^2 \lambda) - 1}}.$$

A.5 Disaster risk probabilities

This section contains details about the disaster risk model in Figure 2. Let $F(\cdot)$ denote the CDF of Δc . [Backus et al. \(2011, p. 1976\)](#) show that

$$F(-b) = \sum_{j=0}^{\infty} \Phi\left(\frac{-b - \mu - j\theta}{\sqrt{\sigma^2 + j\nu^2}}\right) \cdot \frac{e^{-\kappa} \kappa^j}{j!}, \quad (\text{A.14})$$

where $\Phi(\cdot)$ is the CDF of a standard normal distribution. From here it is straightforward to compute the physical CDF of return on equity, $R = \exp(\lambda\Delta c)$, by a change of variables and truncating the sum in (A.14). Secondly, to obtain the risk-neutral CDF, I use the result of [Backus et al. \(2011, p. 1987\)](#) that the risk-neutral distribution of Δc is the same as in (A.14), with new parameters

$$\tilde{\kappa} = \kappa e^{-\gamma\theta + (\gamma\nu)^2/2}, \quad \tilde{\theta} = \theta - \gamma\nu^2.$$

It follows that $\tilde{\kappa} > \kappa$ if $\theta < 0$ (more jumps) and $\tilde{\theta} < \theta$ (outcomes of jump is more negative on average). This explains the fat left tail of the risk-neutral distribution in Figure 2. The quantile bound, HJ bound and SDF volatility can now easily be calculated from the expression for the physical and risk-neutral distribution.

A.6 Formulas for market moments

This Section presents formulas for the (un)truncated risk-neutral moments of the excess market return. An alternative way to calculate these moments is provided by [Chabi-Yo and Loudis \(2020, Appendix B\)](#). I use a slight abuse of notation and write $\tilde{Q}(\tau) := \tilde{Q}_\tau(R_{m,t \rightarrow N})$, to emphasize that the integrals below are taken with respect

to τ .

Proposition A.3. *Any risk-neutral moment can be computed from the risk-neutral quantile function, since*

$$\tilde{\mathbb{E}}_t [(R_{m,t \rightarrow N} - R_{f,t \rightarrow N})^n] = \int_0^1 [\tilde{Q}_\tau (R_{m,t \rightarrow N} - R_{f,t \rightarrow N})]^n d\tau = \int_0^1 [\tilde{Q}(\tau) - R_{f,t \rightarrow N}]^n d\tau. \quad (\text{A.15})$$

Moreover, any truncated risk-neutral moment can be calculated by

$$\tilde{\mathbb{E}}_t [(R_{m,t \rightarrow N} - R_{f,t \rightarrow N})^n \mathbb{1}(R_{m,t \rightarrow N} \leq k_0)] = \int_0^{\tilde{F}_t(k_0)} [\tilde{Q}(\tau) - R_{f,t \rightarrow N}]^n d\tau.$$

Remark. Frequently I use $k_0 = \tilde{Q}_\tau$, in which case the truncated moment formula reduces to

$$\tilde{\mathbb{E}}_t \left[(R_{m,t \rightarrow N} - R_{f,t \rightarrow N})^n \mathbb{1}(R_{m,t \rightarrow N} \leq \tilde{Q}_\tau) \right] = \int_0^\tau [\tilde{Q}(p) - R_{f,t \rightarrow N}]^n dp.$$

Proof. For any random variable X and integer n such that the n -th moment exists, we have

$$\mathbb{E}[X^n] = \int_0^1 [Q_X(\tau)]^n d\tau.$$

This follows straightforward from the substitution $x = Q(\tau)$. Now use that for any constant $a \in \mathbb{R}$, $Q_{X-a}(\tau) = Q_X(\tau) - a$ to derive (A.15). The truncated formula follows similarly. \blacksquare

A.7 Proof of Theorem 4.3 and Corollary 4.4

Before I prove Theorem 4.3 and Corollary 4.4, I collect several results about the SDF in representative agent models.

Lemma A.4. *Assume a representative agent model with SDF given by (4.10), then*

$$\tau - F_t(\tilde{Q}_{t,\tau}) = -\frac{\widetilde{\text{COV}}_t \left[\mathbb{1}(R_{m,t \rightarrow N} \leq \tilde{Q}_{t,\tau}), \zeta(R_{m,t \rightarrow N}) \right]}{\widetilde{\mathbb{E}}_t [\zeta(R_{m,t \rightarrow N})]}, \quad (\text{A.16})$$

where $\zeta(\cdot)$ is defined in (4.11).

Proof. Use the reciprocal of the SDF to pass from physical to risk-neutral measure

$$\begin{aligned} F_t(\tilde{Q}_{t,\tau}) &= \mathbb{E}_t \left[\mathbb{1}(R_{m,t \rightarrow N} \leq \tilde{Q}_{t,\tau}) \right] = \widetilde{\mathbb{E}}_t \left[\mathbb{1}(R_{m,t \rightarrow N} \leq \tilde{Q}_{t,\tau}) \frac{\mathbb{E}_t [M_{t \rightarrow N}]}{M_{t \rightarrow N}} \right] \\ &= \widetilde{\text{COV}}_t \left[\mathbb{1}(R_{m,t \rightarrow N} \leq \tilde{Q}_{t,\tau}), \frac{\mathbb{E}_t [M_{t \rightarrow N}]}{M_{t \rightarrow N}} \right] + \tau. \end{aligned} \quad (\text{A.17})$$

Rearranging the above and using the definition of $\zeta(\cdot)$, as well as (4.10), we obtain (A.16). \blacksquare

Before I proceed, recall the definition of G in Assumption 4.2:

$$G(x) = \frac{(x - R_{f,t \rightarrow N})^4}{4!} \int_0^1 \zeta^{(4)}(R_{f,t \rightarrow N} + s(x - R_{f,t \rightarrow N})) (1 - s)^3 ds.$$

Under Assumption 4.2, it follows that $G(x) \leq 0$ and I use this fact in Lemma A.7 below. In the proofs that follow, I repeatedly use Taylor's theorem with integral remainder, which I state for completeness.

Theorem A.5. *Let $\zeta^{(k)}(\cdot)$ be absolutely continuous on the closed interval between a and x , then*

$$\zeta(x) = \sum_{k=0}^3 \frac{\zeta^{(k)}(a)}{k!} (x - a)^k + \int_a^x \frac{\zeta^{(4)}(t)}{4!} (x - t)^3 dt.$$

Lemma A.6. *Under Assumption 4.2,*

$$\tilde{\mathbb{E}}_t [\zeta(R_{m,t \rightarrow N})] \leq \sum_{k=0}^3 \theta_k \tilde{\mathbb{M}}_{t \rightarrow N}^{(k)} = 1 + \sum_{k=1}^3 \theta_k \tilde{\mathbb{M}}_{t \rightarrow N}^{(k)}.$$

Proof. In the integral of Theorem A.5, substitute $s = (t - a)/(x - a)$ to get

$$\begin{aligned} \zeta(x) &= \sum_{k=0}^3 \frac{\zeta^{(k)}(a)}{k!} (x - a)^k + (x - a)^4 \int_0^1 \frac{\zeta^{(4)}(a + s(x - a))}{4!} (1 - s)^3 ds \\ &\leq \sum_{k=0}^3 \frac{\zeta^{(k)}(a)}{k!} (x - a)^k, \end{aligned}$$

since $\zeta^{(4)}(x) < 0$ by Assumption 4.2. Using this result and taking expectations, I obtain

$$\tilde{\mathbb{E}}_t [\zeta(R_{m,t \rightarrow N})] \leq \sum_{k=0}^3 \theta_k \tilde{\mathbb{M}}_{t \rightarrow N}^{(k)}.
$$\blacksquare$$$$

I now prove Theorem 4.3 and Corollary 4.4.

Proof of Theorem 4.3 and Corollary 4.4. Using Taylor's theorem A.5, I obtain

$$\begin{aligned}
& -\widetilde{\mathbb{COV}}_t \left[\mathbb{1} \left(R_{m,t \rightarrow N} \leq \tilde{Q}_{t,\tau} \right), \zeta(R_{m,t \rightarrow N}) \right] = \\
& \sum_{k=1}^3 \theta_k \left(\tau \tilde{\mathbb{M}}_{t \rightarrow N}^{(k)} - \tilde{\mathbb{M}}_{t \rightarrow N}^{(k)}[\tilde{Q}_{t,\tau}] \right) - \widetilde{\mathbb{COV}}_t \left[\mathbb{1} \left(R_{m,t \rightarrow N} \leq \tilde{Q}_{t,\tau} \right), G(R_{m,t \rightarrow N}) \right] \\
& \geq \sum_{k=1}^3 \theta_k \left(\tau \tilde{\mathbb{M}}_{t \rightarrow N}^{(k)} - \tilde{\mathbb{M}}_{t \rightarrow N}^{(k)}[\tilde{Q}_{t,\tau}] \right).
\end{aligned} \tag{A.18}$$

The last line follows from Lemma A.7 below. Hence,

$$\begin{aligned}
\tau - F_t(\tilde{Q}_{t,\tau}) &= -\frac{\widetilde{\mathbb{COV}}_t \left[\mathbb{1} \left(R_{m,t \rightarrow N} \leq \tilde{Q}_{t,\tau} \right), \zeta(R_{m,t \rightarrow N}) \right]}{\tilde{\mathbb{E}}_t [\zeta(R_{m,t \rightarrow N})]} \\
&\geq \frac{\sum_{k=1}^3 \theta_k \left(\tau \tilde{\mathbb{M}}_{t \rightarrow N}^{(k)} - \tilde{\mathbb{M}}_{t \rightarrow N}^{(k)}[\tilde{Q}_{t,\tau}] \right)}{1 + \sum_{k=1}^3 \theta_k \tilde{\mathbb{M}}_{t \rightarrow N}^{(k)}},
\end{aligned}$$

where the first identity follows from Lemma A.4 and the inequality follows from (A.18) and Lemma A.6. Therefore,

$$\begin{aligned}
Q_{t,\tau} - \tilde{Q}_{t,\tau} &\stackrel{(4.9)}{\approx} \frac{\tau - F_t(\tilde{Q}_{t,\tau})}{\tilde{f}_t(\tilde{Q}_{t,\tau})} \\
&\geq \frac{1}{\tilde{f}_t(\tilde{Q}_{t,\tau})} \left(\frac{\sum_{k=1}^3 \theta_k \left(\tau \tilde{\mathbb{M}}_{t \rightarrow N}^{(k)} - \tilde{\mathbb{M}}_{t \rightarrow N}^{(k)}[\tilde{Q}_{t,\tau}] \right)}{1 + \sum_{k=1}^3 \theta_k \tilde{\mathbb{M}}_{t \rightarrow N}^{(k)}} \right).
\end{aligned} \tag{A.19}$$

If additionally (4.15) holds, then

$$\theta_1 = \frac{1}{R_{f,t \rightarrow N}}, \theta_2 = -\frac{1}{R_{f,t \rightarrow N}^2}, \text{ and } \theta_3 = \frac{1}{R_{f,t \rightarrow N}^3}.$$

Using this in (A.19) gives

$$Q_{t,\tau} - \tilde{Q}_{t,\tau} \geq \frac{1}{\tilde{f}_t(\tilde{Q}_{t,\tau})} \left(\frac{\sum_{k=1}^3 \frac{(-1)^{k+1}}{R_{f,t \rightarrow N}^k} \left(\tau \tilde{\mathbb{M}}_{t \rightarrow N}^{(k)} - \tilde{\mathbb{M}}_{t \rightarrow N}^{(k)}[\tilde{Q}_{t,\tau}] \right)}{1 + \sum_{k=1}^3 \frac{(-1)^{k+1}}{R_{f,t \rightarrow N}^k} \tilde{\mathbb{M}}_{t \rightarrow N}^{(k)}} \right).$$

■

Lemma A.7. Suppose that Assumption 4.2. In addition, define τ^* so that $G(\tilde{Q}_{t,\tau^*}) = G(R_{m,t \rightarrow N})$. Then for all $\tau \leq \tau^*$,

$$\widetilde{\mathbb{COV}}_t \left[\mathbb{1} \left(R_{m,t \rightarrow N} \leq \tilde{Q}_{t,\tau} \right), G(R_{m,t \rightarrow N}) \right] \leq 0. \tag{A.20}$$

Proof. If $\zeta^{(4)} \equiv 0$, then (A.20) trivially holds for all τ . Hence, assume that $\zeta^{(4)}$ is not identically equal to zero. Rewrite the covariance in (A.20) as

$$\Gamma(\tau) = \tilde{\mathbb{E}}_t \left[\left(\mathbb{1}(R_{m,t \rightarrow N} \leq \tilde{Q}_{t,\tau}) - \tau \right) G(R_{m,t \rightarrow N}) \right].$$

Notice that $\Gamma(\tau) \rightarrow 0$ as $\tau \rightarrow 0$ due to the Cauchy-Schwarz inequality and $\mathbb{1}(R_{m,t \rightarrow N} \leq \tilde{Q}_{t,\tau})$ is Bernoulli with variance $\tau(1 - \tau)$. Differentiate with respect to τ and using Leibniz' rule, I get

$$\Gamma'(\tau) = G(\tilde{Q}_{t,\tau}) - \underbrace{\tilde{\mathbb{E}}_t [G(R_{m,t \rightarrow N})]}_{<0}, \quad (\text{A.21})$$

The right most term is negative due to Assumption 4.2. Define τ^* as the smallest $\tau > 0$ such that $\Gamma'(\tau^*) = 0$. Notice that we can always find such a number, since the right most term in (A.21) is independent of τ , while the first term on the right goes to some number smaller than $\tilde{\mathbb{E}}_t [G(R_{m,t \rightarrow N})]$ (by (4.12)) and $G(\tilde{Q}_{t,\tau_1}) = 0$ if $\tilde{Q}_{t,\tau_1} = R_{f,t \rightarrow N}$. Hence, by the intermediate value theorem there exists a $\tau^* > 0$ such that $\Gamma(\tau^*) = 0$. \blacksquare

A.7.1 Verifying the assumptions in representative agent models

The proof of Theorem 4.3 relies on Assumption 4.2. I verify that this Assumption holds for log and CRRA utility, but not for CARA utility.

A.7.2 Log utility

In this case $u(x) = \log x$. It follows that $\zeta(x) = x/R_{f,t \rightarrow N}$. Clearly $\zeta^{(4)}(x) = 0$ and Assumption 4.2 holds.

A.7.3 CRRA utility

In this case, $u(x) = \frac{x^{1-\gamma}}{1-\gamma}$ and assume $\gamma > 1$. It follows that $\zeta(x) = (\frac{x}{R_{f,t \rightarrow N}})^\gamma$ and hence

$$\zeta^{(4)}(x) = \frac{1}{R_{f,t \rightarrow N}^\gamma} \gamma(\gamma-1)(\gamma-2)(\gamma-3)x^{\gamma-4}.$$

Part (ii) of Assumption 4.2 holds if $\gamma \in (0, 1)$. Part (iii) further restricts the risk-aversion coefficient. To see this, observe that the integral in (4.12) is proportional to

$$-\int_0^1 (1-s)^{\gamma-1} ds.$$

This integral goes to $-\infty$ the closer γ gets to 1. Hence, if γ is sufficiently close to 1, condition (iii) holds and if $\gamma = 1$ we recover the log utility case.

A.7.4 CARA utility

In this case, $u(x) = 1 - e^{-\gamma x}$ and $\zeta(x) = e^{\gamma^*(x - R_{f,t \rightarrow N})}$, where $\gamma^* = W_t \gamma$. Since $\zeta^{(4)} > 0$, Assumption 4.2 does not hold.

A.8 Derivation of Gâteaux derivative

In this Section I derive (4.8). For ease of exposition, I drop the time subscripts. For $\lambda \in [0, 1]$, define $\tilde{F}_\lambda := (1 - \lambda)\tilde{F} + \lambda F$. The following (trivial) identity will prove helpful²⁴

$$\tau = \tilde{F}_\lambda \tilde{F}_\lambda^{-1}. \quad (\text{A.22})$$

To further simplify notation, write $q(\lambda) := \tilde{F}_\lambda^{-1}$. Then (A.22) becomes

$$\tau = (1 - \lambda)\tilde{F}(q(\lambda)) + \lambda F(q(\lambda)).$$

Applying the implicit function theorem, we obtain

$$q'(\lambda) = -\frac{-\tilde{F}(q(\lambda)) + F(q(\lambda))}{(1 - \lambda)\tilde{f}(q(\lambda)) + \lambda f(q(\lambda))}.$$

Plug in $\lambda = 0$ to get

$$q'(0) = -\frac{-\tilde{F}(q(0)) + F(q(0))}{\tilde{f}(q(0))}. \quad (\text{A.23})$$

Notice that

$$\tilde{F}_\lambda|_{\lambda=0} = \tilde{F} \implies q(\lambda)|_{\lambda=0} = q(0) = \tilde{F}^{-1}. \quad (\text{A.24})$$

Substitute (A.24) into (A.23) to obtain

$$q'(0) = -\frac{-\tilde{F}(\tilde{F}^{-1}) + F(\tilde{F}^{-1})}{\tilde{f}(\tilde{F}^{-1})} = \frac{\tau - F(\tilde{F}^{-1})}{\tilde{f}(\tilde{F}^{-1})}. \quad (\text{A.25})$$

Notice that $q'(0)$ is exactly equal to the Gâteaux derivative from the definition in (4.7), since

$$\frac{\partial}{\partial \lambda} \varphi \left[(1 - \lambda)\tilde{F} + \lambda F \right] \Big|_{\lambda=0} = \frac{\partial}{\partial \lambda} q(\lambda) \Big|_{\lambda=0} = q'(0).$$

A.9 Proof of Proposition 4.6

Proof. By definition

$$\tau = \mathbb{P}_t(R_{m,t \rightarrow N} \leq Q_{t,\tau}) = \mathbb{P}_t \left(\exp \left(-\frac{1}{2} \sigma_t^2 \lambda + \sigma_t \sqrt{\lambda} Z_{t+N} \right) \leq \exp(-\mu \lambda) Q_{t,\tau} \right).$$

²⁴This “equality” may actually only be an inequality for some τ , but this is immaterial to the argument.

Similarly

$$\tau = \tilde{\mathbb{P}}_t(R_{m,t \rightarrow N} \leq \tilde{Q}_{t,\tau}) = \tilde{\mathbb{P}}_t \left(\exp \left(-\frac{1}{2} \sigma_t^2 \lambda + \sigma_t \sqrt{\lambda} Z_{t+N} \right) \leq \exp(-r_f \lambda) \tilde{Q}_{t,\tau} \right).$$

As a result

$$e^{(\mu - r_f) \lambda} \tilde{Q}_{t,\tau} = Q_{t,\tau}. \quad (\text{A.26})$$

Recall that the quantile regression estimator is equivariant to reparametrization of design: for any 2×2 nonsingular matrix A , we have

$$\hat{\beta}(\tau; R, XA) = A^{-1} \hat{\beta}(\tau; R, X).$$

By Equation (A.26),

$$X(\tau) = \tilde{X}(\tau) \times \underbrace{\begin{bmatrix} 1 & 0 \\ 0 & e^{(\mu - r_f) \lambda} \end{bmatrix}}_{:=A}.$$

Therefore

$$\hat{\beta}(\tau; R, X(\tau)) = \hat{\beta}(\tau; R, \tilde{X}(\tau)A) = A^{-1} \hat{\beta}(\tau; R, \tilde{X}(\tau)).$$

Hence, the predicted quantile using the physical quantile regression (4.26) equals

$$\begin{aligned} [1 & \ Q_{T+1,\tau}(R_{T+2})] \hat{\beta}(\tau; R, X(\tau)) &= [1 \ Q_{T+1,\tau}(R_{T+2})] A^{-1} \hat{\beta}(\tau; R, \tilde{X}(\tau)) \\ &= [1 \ \tilde{Q}_{T+1,\tau}(R_{T+2})] \hat{\beta}(\tau; R, \tilde{X}(\tau)). \end{aligned}$$

This last expression is exactly (4.27). ■

B Estimating the risk-neutral quantile function

B.1 Data description

To estimate the risk-neutral quantile curve for each point in time, I use daily option prices from OptionMetrics covering the period 01-01-1996 until 12-31-2021. This consists of European Put and Call option data on the S&P 500 index. The option contract further contains information on the highest closing bid and lowest closing ask price and price of the forward contract on the underlying security. I use the midpoint of the bid and ask price to proxy for the unobserved option price. In addition, I obtain data on the daily risk-free rate from Kenneth French's website.²⁵ Finally, I obtain stock price data on the closing price of the S&P 500 from WRDS.

²⁵See http://mba.tuck.dartmouth.edu/pages/faculty/ken.french/data_library.html#Research

I use an additional cleaning procedure for the option data, prior to estimating the martingale measure. All observations are dropped for which the highest closing bid price equals zero, as well as all option prices that violate no-arbitrage bounds. Subsequently, I drop all option prices with maturity less than 7 days or greater than 500 days. After the cleaning procedure, I'm left with 23,264,113 option-day observations.

B.2 Estimating the risk-neutral quantile function

There is a substantial literature on how to extract the martingale measure from option prices. I use the *RND Fitting Tool* application on MATLAB, which is developed by [Barletta and Santucci de Magistris \(2018\)](#).²⁶ The tool is based on the orthogonal polynomial expansion of [Filipović et al. \(2013\)](#). In short, the idea is to approximate the conditional risk-neutral density function by an expansion of the form

$$\tilde{f}_t(x) \approx \phi(x) \left[1 + \sum_{k=1}^K \sum_{i=0}^k c_k w_{i,k} x^k \right],$$

where $\phi(x)$ is an arbitrary density and the polynomial term serves to tilt the density function towards the risk-neutral distribution. Further details about the estimation of the coefficients $w_{i,k}$ and c_k can be found in [Filipović et al. \(2013\)](#).

For my purpose, I need to choose the kernel function $\phi(\cdot)$, the estimation method for c_k and the degree of the expansion K . I follow the recommendation of [Barletta and Santucci de Magistris \(2018\)](#) and use the *double beta* distribution for the kernel and principal component analysis to estimate c_k . This is the most robust method for S&P500 options. To avoid overfitting, I use $K = 3$ if the number of option data is less than 70, $K = 6$ if the number is less than 100 and $K = 8$ otherwise. This choice renders a good approximation for most time periods.

I interpolate the estimated risk-neutral densities for a given time period. Occasionally, there are no two interpolation points. In such cases, I drop the observations to avoid negative density estimates due to extrapolation. Since the RND Fitting Tool is designed for an equal number of put and call options, I use Put-Call parity to convert in-the-money call prices to put prices and vice versa. Subsequently, I use Black-Scholes implied volatilities to interpolate the Call-Put option price curve near the forward price. This transformation ensures that the risk-neutral density does not have a discontinuity for strike prices that are close to being at-the-money ([Figlewski, 2010](#)). Finally, I integrate the density function and take the inverse to obtain the risk-neutral quantile curve.

²⁶The application can be downloaded from the author's GITHUB page: <https://github.com/abarletta/rndfittool>

C Crash probability in representative agent models

In this Section, I derive several results about disaster probabilities in representative agent models.

C.1 Crash probability with log utility

Chabi-Yo and Loudis (2020, Remark 1) show that their bounds on the equity premium equal the bounds of Martin (2017) when the representative agent has log preferences. Here, I derive the analogous result for the subjective crash probability of a log investor reported by Martin (2017, Result 2). In our notation, Martin (2017) shows that

$$\mathbb{P}_t(R_{m,t \rightarrow N} < \alpha) = \alpha \left[\text{Put}'_t(\alpha S_t) - \frac{\text{Put}_t(\alpha S_t)}{\alpha S_t} \right], \quad (\text{C.1})$$

where Put'_t is the derivative of the put option price curve seen as a function of the strike. Under log preferences and using (A.17), it follows that

$$\begin{aligned} \mathbb{P}_t(R_{m,t \rightarrow N} < \tilde{Q}_{t,\tau}) &= \tau + \frac{1}{R_{f,t \rightarrow N}} \widetilde{\mathbb{COV}}_t \left[\mathbb{1} \left(R_{m,t \rightarrow N} \leq \tilde{Q}_{t,\tau} \right), R_{m,t \rightarrow N} \right] \\ &= \tau + \frac{1}{R_{f,t \rightarrow N}} \left(\widetilde{\mathbb{E}}_t \left[\mathbb{1} \left(R_{m,t \rightarrow N} \leq \tilde{Q}_{t,\tau} \right) R_{m,t \rightarrow N} \right] - \widetilde{\mathbb{E}}_t(R_{m,t \rightarrow N}) \widetilde{\mathbb{E}}_t \left(\mathbb{1} \left(R_{m,t \rightarrow N} \leq \tilde{Q}_{t,\tau} \right) \right) \right) \\ &= \frac{1}{R_{f,t \rightarrow N}} \widetilde{\mathbb{E}}_t \left[\mathbb{1} \left(R_{m,t \rightarrow N} \leq \tilde{Q}_{t,\tau} \right) R_{m,t \rightarrow N} \right]. \end{aligned} \quad (\text{C.2})$$

The result now follows upon substituting $\tilde{Q}_\tau = \alpha$, since Martin (2017) shows that (C.2) equals the right hand side of (C.1).

C.2 Crash probability with CRRA utility

I now consider the case in which the representative agent has constant relative risk aversion (CRRA) utility, $u(x) = x^{1-\gamma}/(1-\gamma)$, where γ is the relative risk aversion parameter. First, I show that the excess market return is non-decreasing in γ *regardless* of the distribution of the market return.²⁷ The proof uses the following lemma, which is a special case of the FKG inequality (Hsu and Varadhan, 1999, Theorem 1.3).

Lemma C.1 (Chebyshev sum inequality). *Let X be a random variable and let g, h both be non-increasing or non-decreasing. Then,*

$$\mathbb{E}(g(X)h(X)) \geq \mathbb{E}(g(X))\mathbb{E}(h(X)).$$

The inequality is reversed if one is non-increasing and the other is non-decreasing.

²⁷Cochrane (2005) derives this result when the distribution is lognormal.

Proof. Let X_1, X_2 be IID copies of X and assume that g, h are non-decreasing. It follows that

$$(g(X_1) - g(X_2))(h(X_1) - h(X_2)) \geq 0. \quad (\text{C.3})$$

Taking expectations on both sides completes the proof. The same proof goes through if g, h are non-increasing. If one is non-increasing and the other is non-decreasing, then the inequality in (C.3) is reversed. \blacksquare

Proposition C.2. *Assume that a representative investor has CRRA utility, with $\gamma \geq 0$ and $\mathbb{E}_t [R_{m,t \rightarrow N}^{\gamma+1} \log R_{m,t \rightarrow N}] < \infty$. Then, $\mathbb{E}_t [R_{m,t \rightarrow N}] - R_{f,t \rightarrow N}$, is non-decreasing in γ .*

Proof. According to Chabi-Yo and Loudis (2020, Equation (53)), we have

$$\mathbb{E}_t [R_{m,t \rightarrow N}] - R_{f,t \rightarrow N} = \frac{\tilde{\mathbb{E}}_t [R_{m,t \rightarrow N}^{\gamma+1}]}{\tilde{\mathbb{E}}_t [R_{m,t \rightarrow N}^\gamma]} - R_{f,t \rightarrow N} =: g(\gamma).$$

It is enough to show that $g'(\gamma) \geq 0$ for $\gamma \geq 0$. Taking first order conditions, we need to show that

$$\tilde{\mathbb{E}}_t [R_{m,t \rightarrow N}^{\gamma+1} \log R_{m,t \rightarrow N}] \tilde{\mathbb{E}}_t [R_{m,t \rightarrow N}^\gamma] \geq \tilde{\mathbb{E}}_t [R_{m,t \rightarrow N}^{\gamma+1}] \tilde{\mathbb{E}}_t [R_{m,t \rightarrow N}^\gamma \log R_{m,t \rightarrow N}]. \quad (\text{C.4})$$

Introduce another probability measure \mathbb{P}^* , defined as

$$\mathbb{E}_t^* [Z] := \frac{\tilde{\mathbb{E}}_t [Z R_{m,t \rightarrow N}^\gamma]}{\tilde{\mathbb{E}}_t [R_{m,t \rightarrow N}^\gamma]}. \quad (\text{C.5})$$

We can rewrite (C.4) into

$$\mathbb{E}_t^* [R_{m,t \rightarrow N}^\gamma \log R_{m,t \rightarrow N}] \geq \mathbb{E}_t^* [R_{m,t \rightarrow N}^\gamma] \mathbb{E}_t^* [\log R_{m,t \rightarrow N}]. \quad (\text{C.6})$$

Inequality (C.6) follows from Lemma C.1. \blacksquare

I mimic the steps above to show that the physical distribution differs more from the risk-neutral distribution at every point in the support, whenever risk aversion is increasing.

Proposition C.3. *Assume that a representative investor has CRRA utility, with $\gamma \geq 0$ and $\mathbb{E}_t [R_{m,t \rightarrow N}^\gamma \log R_{m,t \rightarrow N}] < \infty$, then $F_t(x)$ is non-increasing in γ . In particular, $\tau - F_t(\tilde{Q}_{t,\tau})$ is non-decreasing in γ .*

Proof. I start from the relation

$$F_t(x) = \tilde{\mathbb{E}}_t \left[\frac{R_{m,t \rightarrow N}^\gamma}{\tilde{\mathbb{E}}_t [R_{m,t \rightarrow N}^\gamma]} \mathbb{1}(R_{m,t \rightarrow N} \leq x) \right].$$

From first order conditions, we need to show that

$$\begin{aligned} \tilde{\mathbb{E}}_t [\log(R_{m,t \rightarrow N}) \mathbb{1}(R_{m,t \rightarrow N} \leq x) R_{m,t \rightarrow N}^\gamma] \tilde{\mathbb{E}}_t [R_{m,t \rightarrow N}^\gamma] &\leq \\ \tilde{\mathbb{E}}_t [R_{m,t \rightarrow N}^\gamma \mathbb{1}(R_{m,t \rightarrow N} \leq x)] \tilde{\mathbb{E}}_t [\log(R_{m,t \rightarrow N}) R_{m,t \rightarrow N}^\gamma]. \end{aligned}$$

Using the same change of measure as in (C.5), we obtain the equivalent statement

$$\mathbb{E}_t^* [\log(R_{m,t \rightarrow N}) \mathbb{1}(R_{m,t \rightarrow N} \leq x)] \leq \mathbb{E}_t^* [\mathbb{1}(R_{m,t \rightarrow N} \leq x)] \mathbb{E}_t^* [\log R_{m,t \rightarrow N}].$$

This inequality holds, since $\log(x)$ and $\mathbb{1}(x \leq x)$ are respectively increasing and non-increasing, hence the result follows from Lemma C.1. Using the substitution $x \rightarrow \tilde{Q}_{t,\tau}$, it follows that $\tau - F_t(\tilde{Q}_{t,\tau})$, is non-decreasing in γ . \blacksquare

Panel (a) in Figure C1 shows that the lower bound in the CRRA model is tight when $\gamma = 1$, but it is rather conservative for $\gamma = 3$. The influence of the lower bound on the quantile function is shown in Panel (b). The quantile approximation is accurate when $\gamma = 1$, but once more conservative when $\gamma = 3$. In both cases the risk-adjustment term uniformly improves upon the risk-neutral approximation.

C.3 Exponential utility

Here, I assume that the representative agent has exponential utility, $u(x) = 1 - e^{-\gamma^* x}$, where γ^* is the absolute risk aversion. According to Chabi-Yo and Loudis (2020, Equation (55)), the following expression for the equity premium obtains

$$\mathbb{E}_t [R_{m,t \rightarrow N}] - R_{f,t \rightarrow N} = \frac{\tilde{\mathbb{E}}_t [R_{m,t \rightarrow N} e^{\gamma R_{m,t \rightarrow N}}]}{\tilde{\mathbb{E}}_t [e^{\gamma R_{m,t \rightarrow N}}]} - R_{f,t \rightarrow N},$$

where $\gamma = \gamma^* W_t$ is relative risk aversion and W_t represents the agent's wealth at time t . Since there is a one-to-one relation between γ and γ^* , it follows from the results in Section C.2 that the equity premium is increasing in γ^* and so is the distance between the physical and risk-neutral distribution, as measured by: $\tau - F_t(\tilde{Q}_{t,\tau})$.

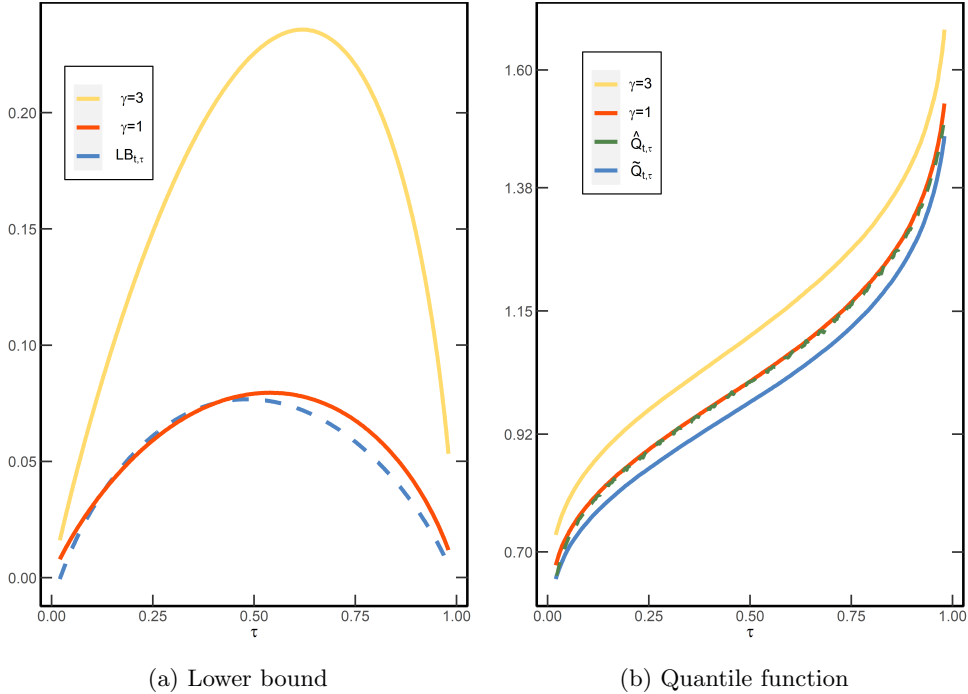


Figure C1: **Lower bound with CRRA utility.** This figure shows the lower bound in a representative agent model with CRRA utility function, $u(x) = x^{1-\gamma}/(1-\gamma)$, for annual returns. The left panel shows $LB_{t, \tau}$ and the true risk-adjustment, $\tau - F_t(\tilde{Q}_{t, \tau})$, for the risk aversion coefficient $\gamma \in \{1, 3\}$. The right panel shows the physical quantile function for $\gamma \in \{1, 3\}$, as well as the proxy for the physical quantile function, $\hat{Q}_{t, \tau} = \tilde{Q}_{t, \tau} + RA_{t, \tau}$, and the risk-neutral quantile function, $\tilde{Q}_{t, \tau}$. The risk-neutral distribution is $\text{Logn} \left[(r - \frac{1}{2}\sigma^2)T, \sigma\sqrt{T} \right]$, where $r = 0, \sigma = 0.2$ and $T = 1$.

D Other SDF bounds

In this Section, I analyze SDF bounds other than the one from [Hansen and Jagannathan \(1991\)](#). For each SDF bound, it is well known under which conditions they are tight. For example, the log bound of [Bansal and Lehmann \(1997\)](#) is known to bind for the growth-optimal portfolio. Under some conditions, the growth-optimal return is equal to the market return. Hence, an approach similar to Section 3.2 can be used to analyze if the market return is growth-optimal. Throughout, I repeatedly use the following identity derived in the proof of the quantile bound

$$\tau = R_f \mathbb{E} \left[M \mathbb{1} \left(R \leq \tilde{Q}_\tau \right) \right]. \quad (\text{D.1})$$

D.1 Bound of [Snow \(1991\)](#)

[Snow \(1991\)](#) derives a continuum of bounds of higher order moments on the SDF. In somewhat simplified form, the idea is to use Hölder's inequality to the defining SDF

equation

$$1 = \mathbb{E}[MR] \leq \mathbb{E}[M^p]^{\frac{1}{p}} \mathbb{E}[R^q]^{\frac{1}{q}},$$

for Hölder exponents $\frac{1}{p} + \frac{1}{q} = 1$ and $p > 1$. Rearranging gives the restriction on the p -th norm of the SDF

$$\mathbb{E}[M^p]^{\frac{1}{p}} \geq \mathbb{E}[R^q]^{-\frac{1}{q}}.$$

The quantile relation (D.1) can similarly be exploited by applying Hölder's inequality on the right hand side, which gives

$$\mathbb{E}[M^p]^{\frac{1}{p}} \geq \left(\frac{\tau}{R_f}\right) \mathbb{E}\left[\mathbb{1}(R \leq \tilde{Q}_\tau)\right]^{-\frac{1}{q}}.$$

D.2 Bound of Bansal and Lehmann (1997)

Here I consider a bound on the logarithm of the SDF. By an application of Jensen's inequality, we get

$$\begin{aligned} 0 = \log(1) &= \log \mathbb{E}[MR] \geq \mathbb{E}[\log M] + \mathbb{E}[\log R] \\ &\implies -\mathbb{E}[\log M] \geq \mathbb{E}[\log R]. \end{aligned}$$

This bound, together with its asset pricing implications, is analyzed in detail by [Bansal and Lehmann \(1997\)](#). It is known to bind for the market portfolio in a representative agent model with log utility. Applying a log transformation to (D.1), we obtain for any $\tau \in (0, 1)$

$$\log(\tau) = \log(R_f) + \log\left(\mathbb{E}\left[M \mathbb{1}(R \leq \tilde{Q}_\tau)\right]\right).$$

Using Jensen's inequality and rearranging gives

$$-\mathbb{E}[\log(M)] \geq \log(R_f) + \mathbb{E}\left[\log\left(\mathbb{1}(R \leq \tilde{Q}_\tau)\right)\right] - \log(\tau).$$

D.3 Bound of Liu (2021)

[Liu \(2021\)](#) develops a continuum of bounds that are based on different moments of the SDF. In particular

$$\mathbb{E}[M^s] \begin{cases} \leq \mathbb{E}\left[R^{-\frac{s}{1-s}}\right]^{1-s}, & \text{if } s \in (0, 1). \\ \geq \mathbb{E}\left[R^{-\frac{s}{1-s}}\right]^{1-s}, & \text{if } s \in (-\infty, 0). \end{cases} \quad (\text{D.2})$$

The proof, as in [Liu \(2021\)](#), follows from an application of the *reverse Hölder inequality*.²⁸ Equality occurs for the return which satisfies

$$\log M = -\frac{1}{1-s} \log R + \text{Constant}.$$

The quantile relation can only be used to obtain the upper bound part in [\(D.2\)](#), since the reverse Hölder inequality requires almost sure positivity of $\mathbb{1}(R \leq \tilde{Q}_\tau)$ to prove the lower bound. For $p \in (1, \infty)$, apply the reverse Hölder inequality to the relation [\(D.1\)](#) to obtain

$$\tau = R_f \mathbb{E} \left[M \mathbb{1} \left(R \leq \tilde{Q}_\tau \right) \right] \geq R_f \mathbb{E} \left[M^{\frac{-1}{p-1}} \right]^{1-p} \mathbb{E} \left[\mathbb{1} \left(R \leq \tilde{Q}_\tau \right)^{\frac{1}{p}} \right]^p$$

Rearranging and using $s := -\frac{1}{p-1} \in (-\infty, 0)$ yields

$$\mathbb{E} [M^s] \geq \left(\frac{\tau}{R_f} \right)^s \mathbb{E} \left[\mathbb{1} \left(R \leq \tilde{Q}_\tau \right) \right]^{1-s}.$$

E Risk-adjustment in the data and in asset pricing models

In this Section, I analyze the approximation to the physical quantile function

$$Q_{t,\tau} \approx \tilde{Q}_{t,\tau} + \frac{\text{LB}_{t,\tau}}{\tilde{f}_t(\tilde{Q}_{t,\tau})} =: \tilde{Q}_{t,\tau} + \text{RA}_{t,\tau}.$$

E.1 Risk-adjustment term in the data

In the empirical application, I compute the risk-adjustment term, $\text{RA}_{t,\tau} = \text{LB}_{t,\tau}/\tilde{f}_t(\tilde{Q}_{t,\tau})$, for the 30, 60 and 90 day horizon. Table [E1](#) contains summary statistics of $\text{RA}_{t,\tau}$. The risk-adjustment term is right-skewed and is most significant for the 5 and 10% quantile. Moreover, over the 30 day horizon, it can spike up to 25% and averages to about 1% in the far left tail. In annual units, this average implies that the risk-neutral and physical quantile differ by 11%, when $\tau = 0.05$.

E.2 Robustness of the risk-adjustment term and risk-neutral quantile

The risk-adjustment term, $\text{RA}_{t,\tau}$, tries to capture the difference between the physical and risk-neutral quantile in the left tail. What are some other measures that are

²⁸The reverse Hölder inequality states that for any $p \in (1, \infty)$ and measure space (S, Σ, μ) that satisfies $\mu(S) > 0$. Then for all measurable real- or complex-valued functions f and g on S such that $g(s) \neq 0$ for μ -almost all $s \in S$, $\|fg\|_1 \geq \|f\|_{\frac{1}{p}} \|g\|_{\frac{-1}{p-1}}$.

Table E1: **Summary statistics risk-adjustment term**

	Horizon (in days)	Mean	Median	Std. dev.	Min	Max
$\tau = 0.05$	30	0.92	0.63	1.07	0.08	24.38
	60	1.81	1.31	1.67	0.1	19.23
	90	2.65	2.02	2.02	0.02	18.63
$\tau = 0.1$	30	0.7	0.45	0.87	0.06	12.22
	60	1.71	1.19	1.66	0.25	19.89
	90	2.86	2.12	2.32	0.04	24.47
$\tau = 0.2$	30	0.47	0.25	0.74	0.04	10.93
	60	1.14	0.69	1.5	0.12	23.57
	90	1.97	1.22	2.33	0.26	28.92

Note: This table reports summary statistics of the risk-adjustment term, $\text{RA}_{t,\tau} = \text{LB}_{t,\tau}/\tilde{f}_t(\tilde{Q}_{t,\tau})$, in (4.21) at different time horizons and different quantile levels over the sample period 2003-2021. All statistics are in percentage point.

available at a daily frequency and contain information about the quantile wedge?

One candidate is the VIX index, which is defined as

$$\text{VIX}^2 = \frac{2R_{f,t \rightarrow N}}{\Delta T} \left[\int_0^{F_t} \frac{1}{K^2} \text{put}_t(K) dK + \int_{F_t}^{\infty} \frac{1}{K^2} \text{call}_t(K) dK \right],$$

where ΔT is the time to expiration, F_t is the forward price on the S&P500, and $\text{put}_t(K)$ (resp. $\text{call}_t(K)$) is the put (resp. call) option price on the S&P 500 with strike K . [Martin \(2017\)](#) shows that VIX measures risk-neutral entropy

$$\text{VIX}^2 = \frac{2}{\Delta T} \tilde{L}_t \left(\frac{R_{m,t \rightarrow N}}{R_{f,t \rightarrow N}} \right),$$

where entropy is defined as $\tilde{L}_t(X) := \log \tilde{\mathbb{E}}_t[X] - \tilde{\mathbb{E}}_t[\log X]$. Entropy, just like variance, is a measure of spread in the distribution. However, entropy places more weight on left tail events than variance, since entropy places more weight on out-of-the money puts. As such, VIX is a good candidate to explain potential differences between $Q_{t,\tau}$ and $\tilde{Q}_{t,\tau}$. Second, the Chicago Board Options Exchange provides daily data on VIX for the 30 day horizon.

Table E2 shows the result of the quantile regression

$$Q_{t,\tau}(R_{m,t \rightarrow N}) - \tilde{Q}_{t,\tau}(R_{m,t \rightarrow N}) = \beta_0(\tau) + \beta_1(\tau)\text{RA}_{t,\tau} + \beta_{\text{VIX}}(\tau)\text{VIX}. \quad (\text{E.1})$$

We see that β_{VIX} is marginally significant in the left tail. In contrast, $\beta_1(\tau)$ is even

more significant compared to Table 3. Furthermore, the explanatory power of the model that only includes VIX is lower compared to the model that only includes $\text{RA}_{t,\tau}$ (Table 3).

Table E2: Quantile regression lower bound and VIX

	$\widehat{\beta}_0(\tau)$	$\widehat{\beta}_1(\tau)$	$\widehat{\beta}_{\text{VIX}}(\tau)$	$R^1(\tau)[\%]$	$R^1(\tau)[\%]$ (VIX only)
$\tau = 0.05$	-0.20 (2.021)	10.09 (0.345)	-0.30 (0.143)	6.34	5.51
$\tau = 0.1$	-0.35 (1.515)	5.06 (0.310)	-0.22 (0.100)	3.41	2.84
$\tau = 0.2$	-0.28 (1.112)	3.62 (0.265)	-0.25 (0.079)	0.61	0.18

Note: This table reports the QR estimates of (E.1) over the 30-day horizon. The sample period is 2003-2021, standard errors are shown in parentheses and calculated using SETBB with a block length of 5 times the forecast horizon. $R^1(\tau)$ denotes the goodness-of-fit measure (4.3). The last column denotes the goodness-of-fit in the model that only uses VIX as covariate. The standard error and point estimate of β_0 is multiplied by 100 for readability.

As a second robustness check, I consider how well the direct quantile forecast, $\widehat{Q}_{t,\tau} = \widetilde{Q}_{t,\tau} + \text{RA}_{t,\tau}$, compares to the VIX forecast. Since $\widehat{Q}_{t,\tau}$ does not require any parameter estimation, this exercise is a measure of out-of-sample performance. However, VIX does not directly measure $Q_{t,\tau}$ and hence I use an expanding window to obtain the VIX benchmark: $\widehat{Q}_{t,\tau}^{\text{VIX}} := \widehat{\beta}_0(\tau) + \widehat{\beta}_1(\tau)\text{VIX}_t$. Finally, I use the following out-of-sample metric to compare both forecasts

$$R_{\text{oos}}^1(\tau) = 1 - \sum_{t=500}^T \rho_\tau(R_{m,t \rightarrow N} - \widehat{Q}_{t,\tau}) / \sum_{t=500}^T \rho_\tau(R_{m,t \rightarrow N} - \widehat{Q}_{t,\tau}^{\text{VIX}}).$$

Notice that $R_{\text{oos}}^1(\tau) > 0$, if $\widehat{Q}_{t,\tau}$ attains a lower error than $\widehat{Q}_{t,\tau}^{\text{VIX}}$. This exercise is more ambitious, since $\widehat{Q}_{t,\tau}^{\text{VIX}}$ makes use of in-sample information. Nonetheless, Figure E2 shows that $\widehat{Q}_{t,\tau}$ outperforms the VIX predictor at all quantile levels.

Figure E3 performs a similar exercise in the right tail, but instead of using $\widehat{Q}_{t,\tau}$, I use $\widetilde{Q}_{t,\tau}$, since Table 2 shows that the risk-neutral quantile is a good approximation to $Q_{t,\tau}$ in the right tail. We see that $\widetilde{Q}_{t,\tau}$ outperforms $\widehat{Q}_{t,\tau}^{\text{VIX}}$ at all quantile levels. Hence, the risk-neutral approximation in the right tail is more accurate than using the in-sample VIX measure.

E.3 Lower bound in Black-Scholes model

This section illustrates the accuracy of the quantile approximation in (4.17) in a discretized version of the Black-Scholes model with time varying parameters. Specif-

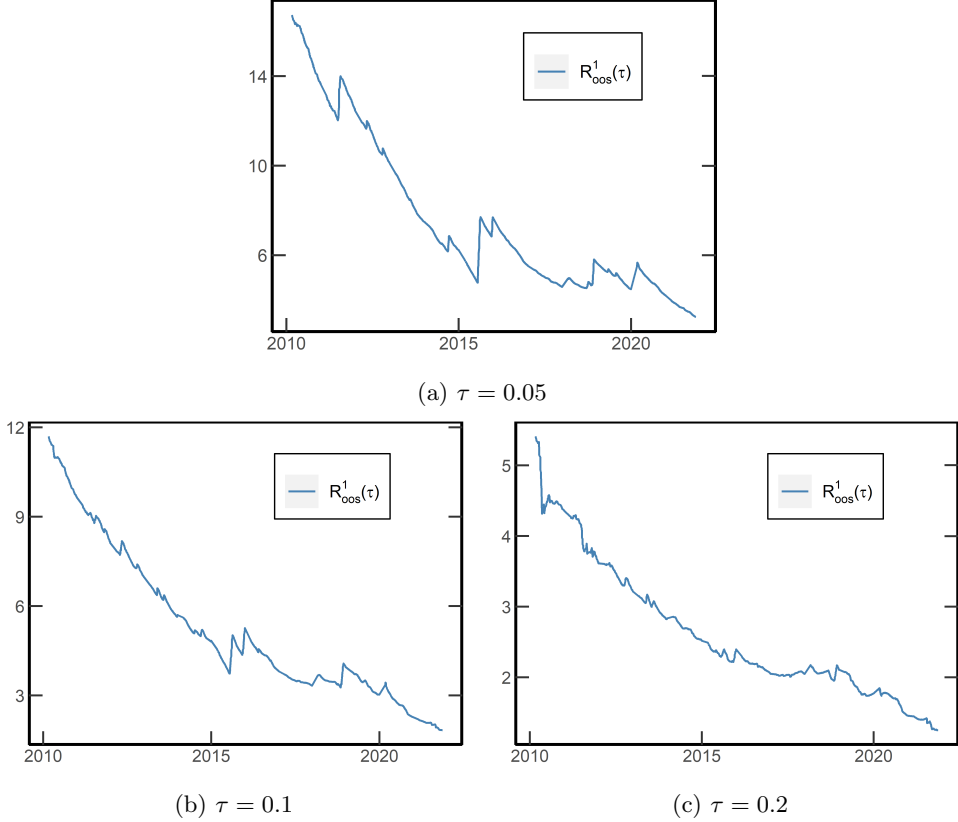


Figure E2: **Out-of-sample forecast using risk-adjusted quantile with VIX benchmark.** This figure shows the cumulative out-of sample $R^1(\tau)$, defined as $R^1_{oos}(\tau) = 1 - \sum_{t=500}^T \rho_\tau(R_{m,t \rightarrow N} - \hat{Q}_{t,\tau}) / \sum_{t=500}^T \rho_\tau(R_{m,t \rightarrow N} - \hat{Q}_{t,\tau}^{\text{VIX}})$, where $\hat{Q}_{t,\tau} = \hat{Q}_{t,\tau} + \text{RA}_{t,\tau}$, $\hat{Q}_{t,\tau}^{\text{VIX}} = \hat{\beta}_0(\tau) + \hat{\beta}_1(\tau) \cdot \text{VIX}_t$, and $\hat{\beta}_0(\tau), \hat{\beta}_1(\tau)$ are the regression estimates from a quantile regression of $R_{m,t \rightarrow N}$ on VIX_t , using data only up to time t . The horizon is 30 days and the QR estimates are dynamically updated using an expanding window over the period 2003–2021. The initial sample uses 500 observations.

ically, I assume the following DGP

$$\begin{aligned}
 R_{m,t \rightarrow N} &= \exp \left(\left(\mu_t - \frac{1}{2} \sigma_t^2 \right) \lambda + \sigma_t \sqrt{\lambda} Z_{t+1} \right), \quad Z_{t+1} \sim N(0, 1) \quad (\text{E.2}) \\
 \sigma_t &\sim \mathbf{Unif}[0.05, 0.35] \\
 \mu_t &\sim \mathbf{Unif}[-0.02, 0.2].
 \end{aligned}$$

The returns under risk-neutral dynamics are given by

$$\tilde{R}_{m,t+1} = \exp \left((r_t - \frac{1}{2} \sigma_t^2) \lambda + \sigma_t \sqrt{\lambda} Z_{t+1} \right) \quad (\text{E.3})$$

$$r_t \sim \mathbf{Unif}[0, 0.03]. \quad (\text{E.4})$$

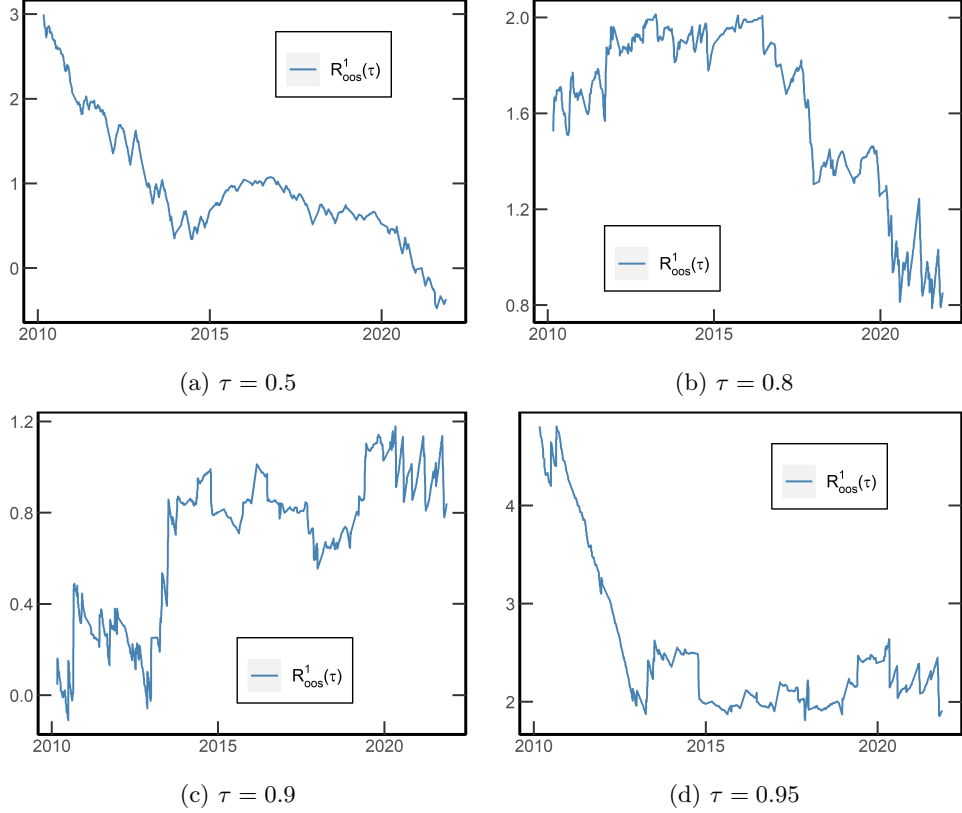


Figure E3: Out-of-sample forecast using risk-neutral quantile with VIX benchmark. This figure shows the cumulative out-of-sample $R^1(\tau)$, defined as $R^1_{oos}(\tau) = 1 - \sum_{t=500}^T \rho_\tau(R_{m,t \rightarrow N} - \hat{Q}_{t,\tau}) / \sum_{t=500}^T \rho_\tau(R_{m,t \rightarrow N} - \hat{Q}_{t,\tau}^{\text{VIX}})$, where $\hat{Q}_{t,\tau}^{\text{VIX}} = \hat{\beta}_0(\tau) + \hat{\beta}_1(\tau) \cdot \text{VIX}_t$, and $\hat{\beta}_0(\tau), \hat{\beta}_1(\tau)$ are the regression estimates from a quantile regression of $R_{m,t \rightarrow N}$ on VIX_t , using data only up to time t . The horizon is 30 days and the QR estimates are dynamically updated using an expanding window over the period 2003–2021. The initial sample uses 500 observations.

Finally, assume that all parameters are IID over time and that options are priced according to the Black-Scholes formula, conditional on time t . In this setup, it is fruitless to use historical data to predict future quantiles, since parameters change unpredictably over time. We use $\lambda = 1/12$ to mimic the monthly application in this paper. It is assumed that the risk-neutral quantile function is known at the start of period t , as it is in the real world, by the result of [Breeden and Litzenberger \(1978\)](#). I use the risk-neutral quantile function to calculate $\text{LB}_{t,\tau}$ at time t . Then, following the approximation in (4.17), the physical quantile function is estimated by

$$\hat{Q}_{t,\tau} = \tilde{Q}_{t,\tau} + \text{RA}_{t,\tau}. \quad (\text{E.5})$$

We take 3,000 return observations that are generated according to (E.2). This exercise is repeated 1,000 times. To assess the accuracy of the approximation in (E.5), I

use several metrics. For every sample, I estimate a quantile regression of the form

$$Q_\tau(R_{t+1}) = \beta_0(\tau) + \beta_1(\tau)\hat{Q}_{t,\tau},$$

where $\hat{Q}_{t,\tau}$ comes from (E.5). The first two columns in Table E3 report the average values of the QR estimates across the 1,000 simulations. The means are rather close to 0 and 1 respectively for all quantiles. If (4.9) is a good approximation, one expects $Q_{t,\tau} > \hat{Q}_{t,\tau}$, since $\text{LB}_{t,\tau} \leq \tau - F_t(\hat{Q}_{t,\tau})$. The third column in Table E3 shows this happens for the majority of samples. The fourth column shows the correlation between $Q_{t,\tau}$ and $\hat{Q}_{t,\tau}$, which is very close to one, and corroborates the view that the approximation is quite accurate. Columns four and five document the percentage of non rejection of H_0 , which is indeed quite high. The last column considers non rejection of the joint null hypothesis, which is also high except for the $\tau = 0.1$ quantile. Overall, Table E3 suggests that (E.5) is a highly accurate predictor of the physical quantile function.

Table E3: Simulation results

	$\mathbb{E}\hat{\beta}_0(\tau)$	$\mathbb{E}\hat{\beta}_1(\tau)$	$Q > \hat{Q}$	$\rho(Q, \hat{Q})$	$H_0 : \hat{\beta}_0(\tau) = 0$	$H_0 : \hat{\beta}_1(\tau) = 1$	$H_0 : [\hat{\beta}_0(\tau), \hat{\beta}_1(\tau)] = [0, 1]$
$\tau = 0.01$	0.01	0.99	0.85	1	0.94	0.96	0.8
$\tau = 0.05$	-0.03	1.04	0.69	0.99	0.9	0.89	0.66
$\tau = 0.1$	-0.06	1.07	0.64	0.99	0.78	0.76	0.47

Note: $\mathbb{E}\hat{\beta}_0(\tau)$ denotes the average QR estimate of $\hat{\beta}_0(\tau)$ and likewise $\mathbb{E}\hat{\beta}_1(\tau)$ shows it for $\hat{\beta}_1(\tau)$. $Q > \hat{Q}$ shows the fraction of times the true physical quantile is larger than our predicted quantile. Columns $H_0 : \hat{\beta}_0(\tau) = 0$ and $H_0 : \hat{\beta}_1(\tau) = 1$ report the fraction of times the individual null hypotheses $\beta_0(\tau) = 0, \beta_1(\tau) = 1$ are not rejected. The last column reports the fraction of times the joint null hypothesis is not rejected.

Example E.1. I illustrate the von Mises approximation (4.9) in the Black-Scholes model with fixed parameters: $\lambda = 1$ (one year), $\mu = 0.08, r = 0.02, \sigma = 0.2$.²⁹ We can explicitly calculate F^{-1}, \tilde{F}^{-1} and \tilde{f} owing to the lognormal assumption. Figure E4 shows the risk-neutral quantile function, von Mises approximation (4.9) and the true physical quantile function. Observe that the approximation (4.9) is very accurate in this case.

E.4 Bias in quantile regression

In the empirical application, we have to estimate $\tilde{Q}_{t,\tau}, \tilde{f}(\cdot)$ and $\text{LB}_{t,\tau}$. Therefore, the estimated coefficients in the quantile regression are biased, due to measurement error in the covariate. I present simulation evidence which shows that the bias is small in finite samples.

²⁹For illustrative purposes, I use $\lambda = 1$, instead of $\lambda = 1/12$, otherwise the physical quantile function and von Mises approximation are indistinguishable.

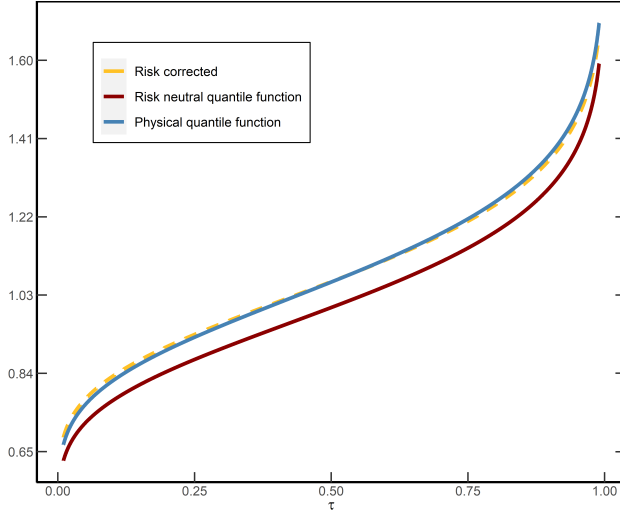


Figure E4: Illustration of quantile approximation (E.5) in the Black-Scholes model.

The setup is as follows. We simulate returns according to model (E.2) and assume that options are priced according to the [Black and Scholes \(1973\)](#) formula at the start of period t . We want to calculate the risk-adjustment term for a maturity of 90 days. As in the empirical application, I assume that options with an exact 90 day maturity are not available, but instead we observe options with maturity 85 and 97 days. I generate a total of 1,000 options every time period with maturities randomly sampled from 85 and 97 days.³⁰ These numbers are roughly consistent with the latter part of our empirical sample. The procedure is repeated for a total of 1,000 time periods. For the entire sample, I compare the estimated and analytical risk-adjustment term, which respectively are given by

$$\begin{aligned} \text{RA}_{t,\tau}^e &:= \widehat{\tilde{Q}}_{t,\tau} + \frac{\widehat{\text{LB}}_{t,\tau}}{\widehat{f}_t(\widehat{\tilde{Q}}_{t,\tau})} \\ \text{RA}_{t,\tau}^a &:= \tilde{Q}_{t,\tau} + \frac{\text{LB}_{t,\tau}}{\tilde{f}_t(\tilde{Q}_{t,\tau})}. \end{aligned}$$

The hats in $\text{RA}_{t,\tau}^e$ signify that the risk-neutral quantile, PDF and lower bound are estimated from the available options at time t , using the procedure in [Appendix B.2](#). The terms in $\text{RA}_{t,\tau}^a$ are obtained from the known analytical expression of the risk-neutral distribution (recall (E.3)). I then use QR to estimate the models

$$\begin{aligned} Q(R_{t+1}) &= \widehat{\beta}_0(\tau) + \widehat{\beta}_{1,e}(\tau) \text{RA}_{t,\tau}^e \\ Q(R_{t+1}) &= \widehat{\beta}_0(\tau) + \widehat{\beta}_{1,a}(\tau) \text{RA}_{t,\tau}^a. \end{aligned}$$

³⁰So on average there will 500 options with maturity 85 days and 500 with maturity 97 days.

I use the ratio $\hat{\beta}_{1,e}/\hat{\beta}_{1,a}$ to measure the relative bias in the sample. This is repeated 500 times to get a distribution of the relative bias. Figure E5 shows boxplots of the bias for several quantiles. We see that the relative bias is very small and centered around 1. Hence, the error in measurement problem resulting from estimating the risk-adjustment term is limited.

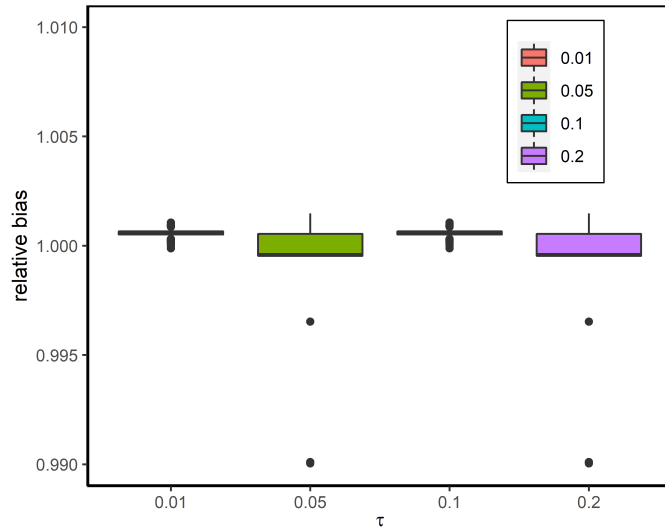


Figure E5: Bias in QR resulting from measurement error.